Monthly Notices
of the
ROYAL ASTRONOMICAL SOCIETY

Mon. Not. R. Astron. Soc. **426,** 91–107 (2012) doi:10.1111/j.1365-2966.2012.21621.x

Confusion limited surveys: using *WISE* to quantify the rarity of warm dust around *Kepler* stars

G. M. Kennedy⋆ and M. C. Wyatt

Institute of Astronomy, University of Cambridge, Madingley Road, Cambridge CB3 0HA

Accepted 2012 June 28. Received 2012 June 28; in original form 2012 May 25

ABSTRACT

We describe a search for infrared excess emission from dusty circumstellar material around 180 000 stars observed by the *Kepler* and *Wide-field Infrared Survey Explorer* missions. This study is motivated by (i) the potential to find bright warm discs around planet host stars, (ii) a need to characterize the distribution of rare warm discs and (iii) the possible identification of candidates for discovering transiting dust concentrations. We find about 8000 stars that have excess emission, mostly at 12 μm. The positions of these stars correlate with the 100 μm background level, so most of the flux measurements associated with these excesses are spurious. We identify 271 stars with plausible excesses by making a 5 MJy sr^{-1} cut in the *IRAS* 100 μm emission. The number counts of these excesses, at both 12 and 22 μm, have the same distribution as extra-Galactic number counts. Thus, although some excesses may be circumstellar, most can be explained as chance alignments with background galaxies. The one exception is a 22 μm excess associated with a relatively nearby A-type star that we were able to confirm because the disc occurrence rate is independent of stellar distance. This detection implies a disc occurrence rate consistent with that found for nearby A-stars. Despite our low detection rate, these results place valuable upper limits on the distribution of large mid-infrared excesses: e.g. fewer than 1:1000 stars have 12 μm excesses ($F_{\rm obs}/F_{\star}$) larger than a factor of 5. In contrast to previous studies, we find no evidence for discs around 1790 stars with candidate planets (we attribute one significant 12 μm excess to a background galaxy), and no evidence that the disc distribution around planet hosts is different from the distribution around the bulk population. Higher resolution imaging of stars with excesses is the best way to rule out galaxy confusion and identify more reliable disc candidates among *Kepler* stars. A similar survey to ours that focuses on nearby stars would be well suited to find the distribution of rare warm discs.

Key words: planets and satellites: formation – circumstellar matter – stars: individual: HIP 13642 – stars: individual: KIC 7345479 – planetary systems.

1 INTRODUCTION

Kepler (Borucki et al. 2003) is revolutionizing our perspective on extra-solar planets (e.g. Holman et al. 2010; Batalha et al. 2011; Doyle et al. 2011; Howell et al. 2011; Lissauer et al. 2011a; Borucki et al. 2012) and will likely yield many Earth-sized planets in the terrestrial zones of their host stars. Like the Solar system, these planetary systems will comprise not only planets, but also smaller objects that for one reason or another did not grow larger. In the Solar system these make up the Asteroid and Kuiper belts, along with other populations such as the Oort cloud, and Trojan and irregular satellites. Characterization of these populations has been critical to building our understanding of how the Solar system formed. For example, one of the primary validation methods of the so-called 'Nice' model for the origin of the outer Solar system's architecture has been the reproduction of these minor body populations and their properties (e.g. Morbidelli et al. 2005; Nesvorný, Vokrouhlický & Morbidelli 2007; Levison et al. 2008).

The exquisite detail with which the Solar system minor body populations are characterized is made clear when they are contrasted with their extra-solar analogues, collectively known as 'debris discs'. First discovered around Vega (Aumann et al. 1984), they are almost always detected by unresolved infrared (IR) emission, visible as an excess above the stellar photosphere. Detection of an excess at multiple wavelengths yields the dust temperature, and thus the approximate radial distance from the star (to within a factor of a few). The radial location can be refined further when spectral

⋆E-mail: gkennedy@ast.cam.ac.uk

features are present (e.g. Lisse et al. 2007). However, because the temperature of a dust or ice grain depends on size, the true radial location (and any radial, azimuthal or vertical structure) can generally only be found by resolved imaging (e.g. Smith & Terrile 1984; Kalas, Graham & Clampin 2005) or interferometry (e.g. Absil et al. 2006; Smith, Wyatt & Haniff 2009).

It is therefore difficult to draw links between the regions of planetary systems occupied by planets and small bodies, and if and how they interact. The best examples of extra-solar systems where known dust and planets are likely to interact are β Pictoris, Fomalhaut and HR 8799 (Burrows et al. 1995; Mouillet et al. 1997; Kalas et al. 2005, 2008; Marois et al. 2008; Su et al. 2009; Moro-Martín et al. 2010). In these cases, the spatial dust distribution is fairly well known because the disc is resolved, but the orbits of the planets, which were only discovered recently with direct imaging, are not. These are rare cases however, and typically the search for links between the major and minor body components of extra-solar planetary systems means asking whether the presence of one makes the presence of the other more or less likely. So far no statistically significant correlation between the presence of planets and debris has been found (Bryden et al. 2009; Kóspál et al. 2009; Dodson-Robinson et al. 2011). However, there is new tentative evidence that nearby stars with low-mass planetary systems are more likely to harbour debris than those with no planet detections (Wyatt et al. 2012), an exciting possibility that has only been achievable recently with better sensitivity to such planetary systems around nearby stars.

One of the key limiting factors in the search for links between debris and planets is the small number of stars known to host both. Two recent *Spitzer* surveys observed about 150 planet host stars, of which about 10 per cent were found to have discs (Bryden et al. 2009; Dodson-Robinson et al. 2011). The small number of disc detections is therefore the product of the number of nearby stars known to host planets that could be observed with *Spitzer*, and the $\sim$10 per cent disc detection rate (for both planet and non-planet host stars). One way to sidestep this problem is therefore to look for discs around a much larger sample of planet host stars, the *Kepler* planet host candidates (Borucki et al. 2011; Batalha et al. 2012).

The method we use to look for discs in this study is to find IR excess emission above that expected from the stellar photosphere. An IR excess is usually interpreted as being thermal emission from an Asteroid or Kuiper-belt analogue, which is heated by the star it orbits. We use photometry from the *Wide-field Infrared Survey Explorer* (*WISE*) mission's (Wright et al. 2010) all-sky catalogue, which is most sensitive to dust in the terrestrial region of Sun-like stars. Three properties of warm dust at these relatively close radial distances provide motivation.

First, this warm dust, if discovered, is located in the vicinity of the planets being discovered with *Kepler*. Currently, only one system, HD 69830, is known to host both a planetary system in the terrestrial region and warm dust (Beichman et al. 2005; Lovis et al. 2006). The origin of this dust is unclear, but given the proximity to the planetary system is plausibly related to it (Lisse et al. 2007; Beichman et al. 2011). Through the discovery of similar systems the links between planets and warm dust can be better understood.

For planets discovered by *Kepler*, the knowledge that a transiting planetary system is almost exactly edge-on provides the second motivational aspect. If planets pass in front of the host star, so will coplanar minor body populations. Indeed, the discovery of systems where multiple planets transit their stars (e.g. Holman et al. 2010; Lissauer et al. 2011a,b) provides striking evidence that the Solar system's near-coplanar configuration is probably typical. While transits of individual small bodes will be impossible to detect, it may be possible to detect concentrated populations that arise from a recent collision (Kenyon & Bromley 2005) or perturbations by planets (Stark 2011). The dust must reside on a fairly close orbit – within a few au – to allow multiple transits within the mission lifetime. Thus, the *WISE* sensitivity to terrestrial dust, and likely difficulties in discerning dust transits from other instrumental and real effects, means that the odds of finding dust transits might be maximized by the prior identification of dusty systems.

Finally, but most importantly, detections of terrestrial dust are rare (e.g. Aumann & Probst 1991; Beichman et al. 2006b; Bryden et al. 2006; Hines et al. 2006). Because only a few such systems are known, their occurrence rate is poorly constrained. More discoveries are therefore needed to add to our understanding of the processes that create it. The collision rate in a debris disc is proportional to the orbital period, so warm terrestrial debris discs decay to undetectable levels rapidly, hence their rarity. Indeed, the few that are known are usually thought to be the result of recent collisions, and thus transient phenomena (e.g. HD 69830, HD 172555, BD +20 307, η Corvi, HD 165014, HD 169666, HD 15407A; Beichman et al. 2005; Song et al. 2005; Wyatt et al. 2007; Lisse et al. 2009, 2012; Moór et al. 2009; Fujiwara et al. 2010, 2012). Possible scenarios include objects thrown into the inner regions of a planetary system from an outer reservoir (Gaidos 1999; Wyatt et al. 2007; Booth et al. 2009; Raymond et al. 2011; Bonsor & Wyatt 2012), or the remnant dust from a single catastrophic collision (Beichman et al. 2005; Song et al. 2005; Weinberger et al. 2011).

Clearly, there are reasons that the discovery of debris in the terrestrial regions of known planetary systems is important. However, because *WISE* is sensitive to the rarest and brightest discs around *Kepler* stars, the third point above is of key importance. As stars become more distant, they and their debris discs become fainter, and the number of background galaxies at these fainter flux levels increases. Thus, the bulk of the stars in the *Kepler* field, which lie at distances of hundreds to thousands of parsecs, may not be well suited to debris disc discovery. Practically, the importance of contamination depends on the galaxy contamination frequency relative to the disc frequency (i.e. only if discs are too rare will they be overwhelmed by contamination). *Therefore, because the occurrence rate of the rare discs that WISE is sensitive to is unknown, whether Kepler stars are a good sample for disc detection with WISE is also unknown.*

Characterizing the occurrence rate of rare bright discs is therefore the main goal of this study, because this very distribution sets what can be discovered. While the sample of *Kepler* stars is not specifically needed for this goal, there is the possibility that the disc occurrence rate is higher for stars that host low-mass planets. Such a trend could make this particular sub-sample robust to confusion, even if the general population is not.

An additional potential issue specific to the *Kepler* field is the importance of the Galactic background. High background regions are sometimes avoided by debris disc observations because they make the flux measurement difficult, and can even mask the presence of otherwise detectable emission. Unfortunately, this issue cannot be avoided for the present study, as the *Kepler* field is necessarily located near the Galactic plane to maximize the stellar density on the sky.

In what follows, we describe our search for warm excesses around $\sim$180 000 stars observed by *Kepler* using the *WISE* catalogue. We first outline the data used in this study in Section 2 and in Section 3 describe our spectral energy distribution (SED) fitting method for finding excesses and the various issues encountered. We discuss the interpretation of these excesses in Section 4, and place our findings

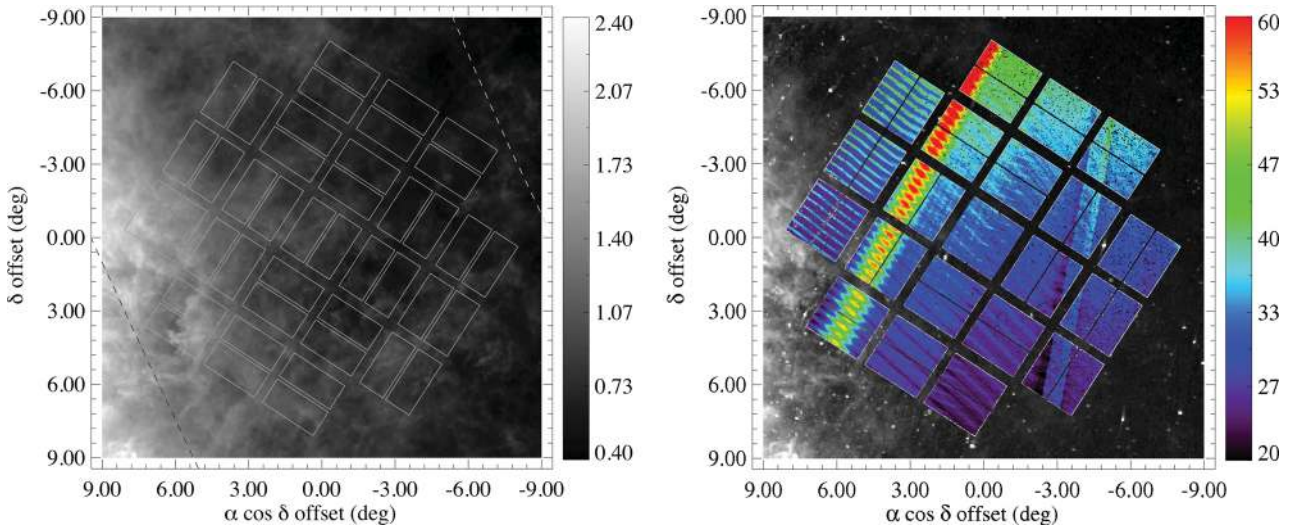

Figure 1. *Kepler* FOV (rectangles) with *IRAS* 100 μm (left-hand panel, scale is $\log \mathrm{MJy\,sr^{-1}}$) and 25 μm (right-hand panel) IRIS maps as background (Miville-Deschênes & Lagache 2005). North is up and east is left. The Galactic plane is towards the south-east, and in the left-hand panel galactic latitudes of 5° and 22° are shown as dashed lines. The *WISE W1* mean pixel coverage in frames (called '`w1cov`' in the catalogue, coloured dots and scale) is shown in the right-hand panel. Nearly all objects are observed by 20–60 frames, those with less or more have the colour at the respective end of the colour scale.

in the context of discs around nearby stars in Section 5. We discuss the disc–planet relation, rarity of warm bright excesses and some future prospects in Section 6 and conclude in Section 7. Readers only interested in the outcome of this search may wish to skip the details described in Sections 2 and 3.

2 CATALOGUES

The *Kepler* mission is observing ∼200 000 stars near the Galactic plane to look for planets by the transit method (Borucki et al. 2003). The *Kepler* field of view (FOV) covers about 100 deg^2 and is rotated by 90° every three months. Not all stars are observed in all quarters, but Fig. 1 shows that the focal plane has four-fold rotational symmetry (aside from the central part), so most will be visible for the mission lifetime. Stars observed by *Kepler* are brighter than about 16th magnitude and selected to maximize the chance of transit detection and follow up (Batalha et al. 2010). The stars are drawn from the Kepler Input Catalogue (KIC), which contains optical photometry, cross-matched Two-Micron All-Sky Survey (2MASS) IDs and stellar parameters for millions of objects within the FOV (Brown et al. 2011).

The entire *Kepler* FOV is covered by the all-sky *WISE* mission (Wright et al. 2010), as shown by the coloured dots in the right-hand panel of Fig. 1. The scanning strategy used by *WISE* means that the sky coverage varies, and is highly redundant at the ecliptic poles (see Jarrett et al. 2011). *WISE* photometry comprises four bands with isophotal wavelengths of 3.4, 4.6, 12 and 22 μm (called *W1–W4*). The sensitivity is fairly well suited to stars observed by *Kepler*, with 5σ sensitivities of 17.1, 15.7, 11.4 and 8 mag for eight frames in *W1–W4* (corresponding to 44, 93, 800 and 5500 μJy, respectively).

2.1 Cross-matching

There were 189 998 unique KIC objects observed in quarters 1–6 of the mission, which we refer to as Kepler OBserved objects,[1] or 'KOBs'. These KOBs are matched with three photometric catalogues: Tycho 2 (Høg et al. 2000), the 2MASS Point Source Catalogue (Skrutskie et al. 2006) and the *WISE* all-sky catalogue (Wright et al. 2010). Matching with 2MASS is straightforward because designations are already given in the KIC. The relevant 189 765 rows were retrieved using Vizier.[2] Tycho 2 objects were matched using a 1 arcsec search radius and retaining only the closest object, again using the Vizier service. This match returned 13 430 objects. The KIC itself contains photometry in SDSS-like bands (*ugriz* each with 1092, 189 383, 189 829, 186 908, 177 293 KOB measurements, respectively) and a *DDO51*-like narrow-band filter centred on 510 nm (with 176 170 measurements). Finally, *WISE* objects are matched using the IPAC Gator service[3] with a radius of 1 arcsec, which returns 181 004 matches. It is these 181 004 objects that are the focus of this study.

3 FINDING EXCESSES

The method used to identify debris disc candidates is fitting stellar atmospheric model SEDs to the available photometry (known as 'SED fitting'). Optical and near-IR bands are used to fit the stellar atmosphere and make predictions of the photospheric flux at longer wavelengths, which are compared to the *WISE* observations. An IR excess indicates the possible presence of thermal emission from circumstellar dust, but can also arise for other reasons; overestimated flux due to a high Galactic background, chance alignment with a background galaxy that has a cooler spectrum than a star and poor photospheric prediction are three examples. Excesses are usually quantified in two ways: the first is the flux ratio in a band B

$$R_B = F_B / F_{\star B}, \tag{1}$$

where F_B is the photometric measurement and $F_{\star B}$ is the photospheric prediction. The flux from the disc is therefore

$$F_{\mathrm{disc},B} = (R_B - 1)\, F_{\star B}. \tag{2}$$

[1] Retrieved from http://archive.stsci.edu/pub/kepler/catalogs/

[2] http://vizier.u-strasbg.fr/viz-bin/VizieR

[3] http://irsa.ipac.caltech.edu/Missions/wise.html

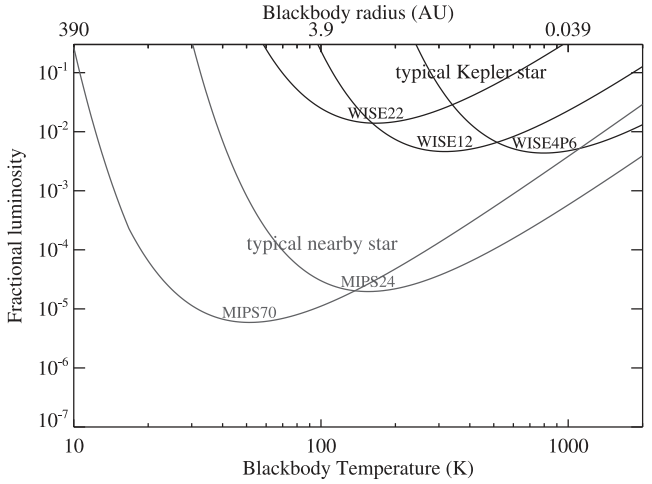

Figure 2. *WISE W2–4* (4.6–22 μm) 3σ sensitivity to blackbody emission around a typical star in the *Kepler* field, a 5460 K star with $K_s = 13.5$ mag (black lines). Also shown is the sensitivity with MIPS at 24 and 70 μm to 55 Cancri, a typical nearby star at 12 pc with $K_s \approx 4.2$ (grey lines).

The second is the excess significance,[4]

$$X_B = \frac{F_B - F_{\star B}}{\sqrt{\sigma_B^2 + \sigma_{\star B}^2}}, \quad (3)$$

where each σ is the photometric or stellar photospheric uncertainty. Typically a star is said to have excess emission when $X_B > 3$, though other (usually higher) values appropriate to the sample in question may be used.

Fig. 2 illustrates the sensitivity of *WISE* to blackbody emission around a 'typical' KOB; a 5460 K star with $K_s = 13.5$ mag. Only discs that have a combination of fractional luminosity ($f = L_{\rm disc}/L_\star$) and temperature that lies above the line for a specific band can be detected in that band. Discs detected at a single wavelength lie somewhere along a single curve similar to (but above) those shown, and may be constrained by non-detections at other wavelengths (e.g. fig. 9 of Bryden et al. 2006). Temperatures can only be derived for discs that lie above multiple lines (i.e. are detected at multiple wavelengths). Compared to the Multiband Imaging Photometer for *Spitzer* (MIPS) observations of the nearby (12 pc) star 55 Cancri (Trilling et al. 2008), the *WISE* sensitivity is much reduced. While MIPS 24 μm observations are generally 'calibration limited' by the precision of the stellar photospheric predictions (i.e. $\sigma_{\star B} \gg \sigma_B$), *WISE* can at best detect a flux ratio of about 50 at 22 μm for the example shown here (so is 'sensitivity limited' and $\sigma_{\star B} \ll \sigma_B$; see Wyatt 2008, for further discussion of sensitivity versus calibration limited surveys). The *WISE* 22 μm observation is actually slightly deeper than the MIPS 24 μm one (both are sensitive to about 1 mJy), so the reason for the difference in disc sensitivity is simply the brightness of the star. The radial scale shows that *WISE* is well suited to finding excesses with large fractional luminosity that lie within the terrestrial planet zone of Sun-like stars. To detect dust at larger distances would require much greater sensitivity and/or longer wavelength data.

Because the sensitivity depends strongly on the brightness of the star, it also varies widely for KOBs. For the nearest and brightest stars the sensitivity is about two orders of magnitude better than shown for the KOB in Fig. 2. However, the longest *WISE* wavelength is 22 μm, so even for the brightest stars the sensitivity to discs cooler than 100 K drops significantly. Therefore, regardless of brightness, the wavelength range of *WISE* and the brightness of most KOBs mean that any detections will be due to very luminous warm excesses. It is less likely that the Wein side of cooler emission will be detected because much higher fractional luminosities are required (i.e. the curves in Fig. 2 rise very steeply to cooler temperatures and larger radii).

3.1 SED fitting

Our SED fitting method uses filter bandpasses to compute synthetic photometry and colour corrections for the stellar models, which are fit to observed photometry by a combination of brute force grids and least-squares minimization. We use Phoenix AMES-Cond models from the *Gaia* grid (Brott & Hauschildt 2005), which cover a wide range of stellar parameters. However, these models only have $T_{\rm eff} < 10\,000$ K, so stars pegged at this temperature are refit with Kurucz models (Castelli & Kurucz 2003). Previous efforts for the *Herschel* (Pilbratt et al. 2010) Disc Emission via a Bias-free Reconnaissance in the Infrared/Submillimetre (DEBRIS) Key Programme (e.g. Matthews et al. 2010) have found that there is little or no difference between these models in terms of photospheric predictions for A-stars.

In addition to being near the Galactic plane, most stars observed by *Kepler* are hundreds to a few thousands of parsecs distant, so are reddened by interstellar dust. The 100 and 25 μm Improved Reprocessing of the *IRAS* Survey (IRIS) maps[5] in Fig. 1 show that cool emission from dust generally increases towards the Galactic plane, but also varies on scales much smaller than the *Kepler* FOV. We correct for this effect using the Rieke & Lebofsky (1985) reddening law.

There are five possible stellar parameters to include in the SED fitting: the effective temperature ($T_{\rm eff}$), surface gravity ($\log g$), metallicity ([M/H]), reddening (A_V), and the solid angle of the star ($\Omega_\star$). The stellar radius $R_\star$ can subsequently be estimated from A_V by adopting some model for Galactic reddening (e.g. Brown et al. 2011) or by assuming the star has a specific luminosity class. In early SED fitting runs where all parameters were left free, models were commonly driven to implausible regions of parameter space in order to minimize the χ^2. Similar issues lead Brown et al. (2011) to use a Bayesian approach, with priors based on observed stellar populations. Rather than duplicate and/or verify their method, we use some of their KIC stellar parameters as described below because our goal is to obtain the best photospheric prediction in *WISE* bands, not to derive stellar parameters.

Verner et al. (2011) show that the KIC gravities systematically differ from those derived by astroseismology by about 0.23 dex, though unfortunately the discrepancy is strongest for those with $\log g > 4$ (i.e. dwarfs). In order to reduce the number of fitted parameters, we therefore fix $\log g$ in our fitting to the KIC value minus 0.23 dex. Where no $\log g$ is tabulated, we set it to 4.5, appropriate for the solar-type stars that make up the bulk of KOBs. To further reduce the number of parameters, we also fix [M/H] to the KIC value.

We use least-squares minimization to find an adequately fitting model, starting with the parameters tabulated in the KIC. When no

[4] This quantity is usually called χ_B, but we instead dub it X_B to avoid confusion with the goodness of fit indicator χ^2. In this study we usually use the term 'excess significance' instead of the symbol.

[5] Retrieved from http://skyview.gsfc.nasa.gov/

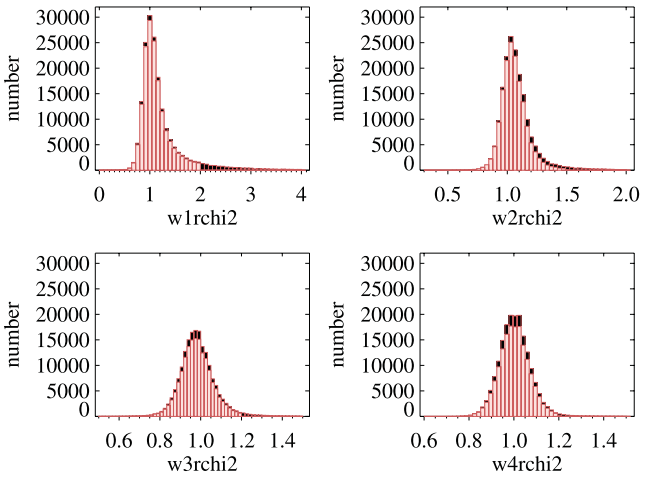

Figure 3. Goodness-of-fit quality for *WISE* source extraction in bands *W1–4* (`w1,2,3,4rchi2`). The non-Gaussian *W1* distribution is an indication of confusion with nearby sources. The black histograms show all *WISE* sources, and the pink histograms show those remaining after the cut in goodness of fit described in the text.

parameters are given (most likely because a good fit could not be found for the KIC; Brown et al. 2011), we do a grid search over $T_{\rm eff}$ and $\Omega_\star$ at $A_V = 0$ to find an initial fit, and then iterate to the best fit with these as free parameters (we apply a cut in fit quality below so if the fits remain poor the stars are excluded.).

We use photometric bands up to and including *WISE W1* to fit the stellar atmosphere. Including *W1* in the stellar fit is reasonable because main-sequence stars rarely show excesses shortwards of about 10 μm. In fact, bands such as *IRAS* 12 μm and *AKARI* 9 μm can usually be used to fit the photosphere, and it is only in rare cases, mostly for A-type stars, that these bands show an excess. In the present case, however, the sample is two to three orders of magnitude larger than a typical debris disc survey, and our goal is to find rare excesses in these bands.

3.1.1 Discarding suspect and poor photometry

Care must be taken when using the photometry from the 2MASS and *WISE* catalogues. The very large number of sources means that small issues that are usually ignored result in hundreds of spurious excesses. Both catalogues have various quantities that can be used to identify and mitigate these problems. These are either flags that indicate contamination, saturation, upper limits, etc., or values that quantify some property such as the goodness of fit achieved in the source extraction. Most issues were uncovered in early SED fitting runs, where the distribution of some catalogue property (source extraction quality for example) was very different for excesses than for the bulk population.

The *WISE* catalogue has several indicators that can be used to remove suspect photometry, which are related to either source extraction or image artefacts.[6] We first consider the reduced χ^2 from the source extraction for each *WISE* bands, whose distributions are shown in Fig. 3 (the columns in the catalogue are called `wXrchi2` where `X` is 1, 2, 3 or 4). These measure the quality of the profile fitting source extraction; a high value is a likely indicator that the source is not well described by a point source, so could be resolved or confused with another object. Any deviation from a point source cannot be due to a resolved debris disc; most *Kepler* stars are hundreds to thousands of parsecs away and *WISE* is sensitive to warm excesses that lie at small stellocentric distances (i.e. have very small angular size)

The most noticeable feature in Fig. 3 is that *W1* shows a non-Gaussian distribution. Given that the difference in beam full-width at half-maximum (FWHM) from *W1* to *W2* is only 6.1 versus 6.4 arcsec and the wavelength difference is small, it seems unlikely that such a large difference in the χ^2 distributions is astrophysical. However, we found that sources with poor *W1* source extraction were more likely to show excesses (above `w1rchi2` of about 2), which we attribute to confusion with nearby sources. Based on this result and the distributions in Fig. 3 we avoid poor source extraction by keeping *WISE* photometry only when the χ^2 is smaller than 2, 1.5, 1.2 and 1.2 in *W1–4*, respectively. A similar, but less stringent cut is also made by only retaining sources where the extension flag (`ext_flg`) is zero, which means that no band has a $\chi^2 > 3$ and the source is not within 5 arcsec of a 2MASS Extended Source Catalogue entry.

The *WISE* catalogue also provides flags (the `cc_flags` column) that note contamination from diffraction, persistence, halo and ghost artefacts. These flags indicate the estimated seriousness of the contamination, whether the artefact may be affecting a real source, or the artefact may be masquerading as a source. We avoid photometry with any indication of contamination (i.e. both types).

Applying these quality criteria to the *WISE* data results in 126 743, 128 610, 78 340 and 9790 detections with a signal-to-noise ratio (S/N) of greater than three in *W1–4*, respectively. A total of 144 655 sources have a *WISE* detection in at least one band.

The 2MASS catalogue also has columns for the profile fitting source extraction χ^2 in each band (called `J,H,Kpsfchi`).[7] Early SED fitting runs found that nearly half of the *W1–2* excesses had a 2MASS reduced $\chi^2 > 2$, particularly in the *J* band. Given that only about 5 per cent of all 2MASS sources matched with KOBs have a *J* band $\chi^2 > 2$, we concluded that the higher *W1* and *W2* excess occurrence rate was related to the poorer 2MASS source extraction. As with the *WISE W1* source extraction we attribute this correlation to confusion. We therefore only use 2MASS data when the χ^2 from source extraction for all three bands is less than 2.

We exclude 2MASS photometry for about 5000 2MASS objects that have the *E*, *F*, *X* or *U* photometric quality flags. The first two flags represent the poorest quality photometry; the third is for detections for which no brightness estimate could be made; and the last is for upper limits.

We also used early SED fitting runs to assess the quality of the photometry in each band. We found that Tycho 2 photometry is poorly suited to the task at hand. While the measurements appear accurate, only a few thousand KOBs are brighter than about 11th magnitude (Batalha et al. 2010), and objects fainter than this have large Tycho 2 uncertainties (see Høg et al. 2000). Because most KOBs are near or beyond the Tycho 2 magnitude limits, their precision is poor and we did not use this photometry.

Finally, we found that the KIC *u* photometry was commonly offset below the photospheric models. Given that only 1092 stars have *u* photometry we also excluded this band from the fitting.

[6] http://wise2.ipac.caltech.edu/docs/release/allsky/expsup/sec2_2a.html

[7] http://www.ipac.caltech.edu/2mass/releases/allsky/doc/sec4_4b.html

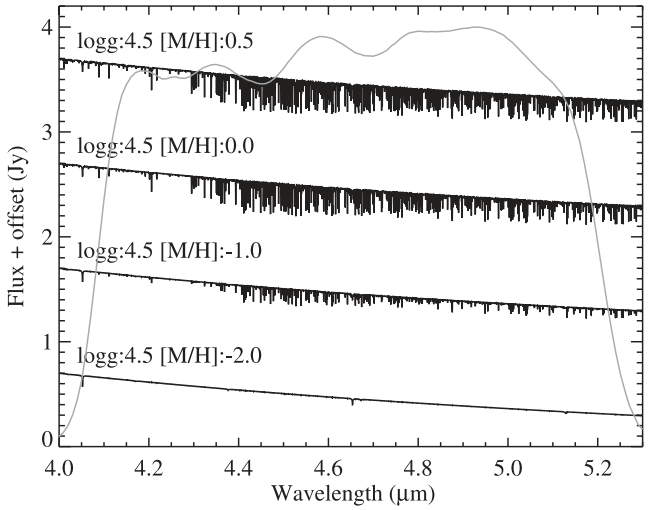

Figure 4. Metallicity-dependent absorption in the *W2* band for $\log g = 4.5$ and a range of [M/H] for a solar-type star. The *W2* bandpass is also shown (arbitrary units, grey line).

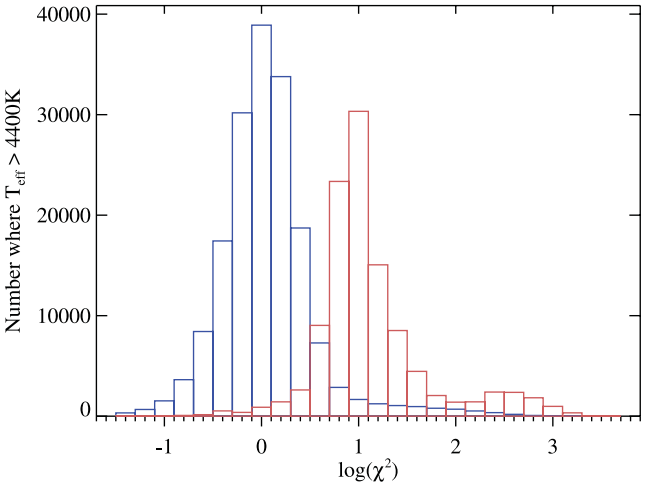

Figure 5. SED reduced χ^2 for stars hotter (filled bars) and cooler (empty bars) than 4400 K (number multiplied by 14). Cooler stars clearly have poorer fits, due to either missing opacity or incorrect bandpasses.

3.1.2 W2 absorption

The *W2* band lies on top of the fundamental CO bandhead, whose depth varies strongly with metallicity for the bulk of our sample. This effect is shown in Fig. 4, where the lines of model spectra within the *W2* bandpass (grey line) become deeper with increasing metallicity. In this plot the flux at the *W2* isophotal wavelength varies by 10 per cent between [M/H] of −2 to +0.5.

As the metallicity increases, the spectrum changes and the colour correction that should be applied to the catalogue (sometimes called 'quoted') flux also increases. Commonly, IR colour corrections are simply taken to be those for a blackbody at the stellar effective temperature. With this approach the examples in Fig. 4 would all have the same colour correction. Thus, inaccuracies in the derived metallicities would lead to a (spurious) trend of larger *W2* excesses for more metal-rich stars. However, when computed properly the colour correction increases with the level of absorption by a similar amount (see also Wright et al. 2010). That is, in the metallicity range considered at 5800 K, the actual fluxes vary by about 10 per cent but the quoted fluxes vary by only 1 per cent. *WISE* is therefore not actually very sensitive to metallicity for Sun-like stars. This sensitivity depends on effective temperature and is strongest for M dwarfs. This conclusion is borne out by the analysis in Section 3.2.

3.1.3 Final photospheric models

The final SED models are generated based on the conclusions of this section. These were computed for all but five of the *WISE* matches (that have no reliable photometry and are identified in the KIC as galaxies). With the photospheric predictions in the *W2–4* bands made based on the optical and near-IR photometry, we now look for excesses.

3.2 Selecting stars with excesses

With a complete set of SEDs, the task of finding excesses is in principle very simple; stars with excesses greater than a sensible significance threshold are selected. In practice this step is complicated by several factors. Atmospheric models for M dwarfs are known to overestimate the stellar flux in the Rayleigh–Jeans regime (e.g. Lawler et al. 2009). Some stars have poor fits and many of these result in excesses that are not real and should be excluded. The sample also contains many giants, whose excesses may be attributed to mass loss rather than a debris disc.

In our sample, there is a clear transition in the quality of the SED fits around 4400 K. Stars cooler than this value have consistently poorer fits than those that are hotter. Such a trend may be due to missing opacity in the stellar atmospheres, but could also be caused by poor filter characterization. Fig. 5 shows χ^2 histograms for the SED fitting, where χ^2 is the reduced sum of squared differences between the photometry and the photospheric model. When split by effective temperature at 4400 K there is a clear difference between the two sets, so we apply a different cut in χ^2 for each; for stars hotter than 4400 K we keep stars with $\chi^2 < 10$, for those cooler than 4400 K we keep stars with $\chi^2 < 100$. We do not simply ignore these cool stars, because the photospheric predictions are generally reliable (though not always, as we find in Section 4.1).

Having made this cut in the quality of the SED fits, Fig. 6 shows the excess significance for bands *W1–4*. Though we have included *W1* in the photospheric fitting, if the photometry in the shorter wavelength bands is of high quality then *W1* will still show an excess if present. The dot colours indicate the gravity derived for the KIC (and used by us with the offset noted above), and show that some *W3–4* excesses are present around stars with lower gravities (i.e. bluer dots around brighter stars with excess significance above 3–4). We therefore remove giants using the criteria of Ciardi et al. (2011), where a star with $T_{\rm eff} > 6000$ is assumed to be a giant if $\log g < 3.5$ and a star with $T_{\rm eff} < 4250$ is assumed to be a giant if $\log g < 4.0$, with a linear transition for intermediate temperatures. Because we have adjusted the gravity of giants as derived in the KIC, we likewise shift their giant criterion down accordingly so our criterion selects the same stars.

A feature present in Fig. 6 for the *W3–4* bands is a flux-dependent cut-off below about 0.5 and 5 mJy, respectively. This cut-off is simply the *WISE* sensitivity limit, which shows that the faintest stars can only be detected if the *W3–4* flux is greater than the photosphere (due to statistical variation or real excess emission).

Having removed poor SED fits and giants, the remaining task in identifying excesses is to set the threshold level of significance.

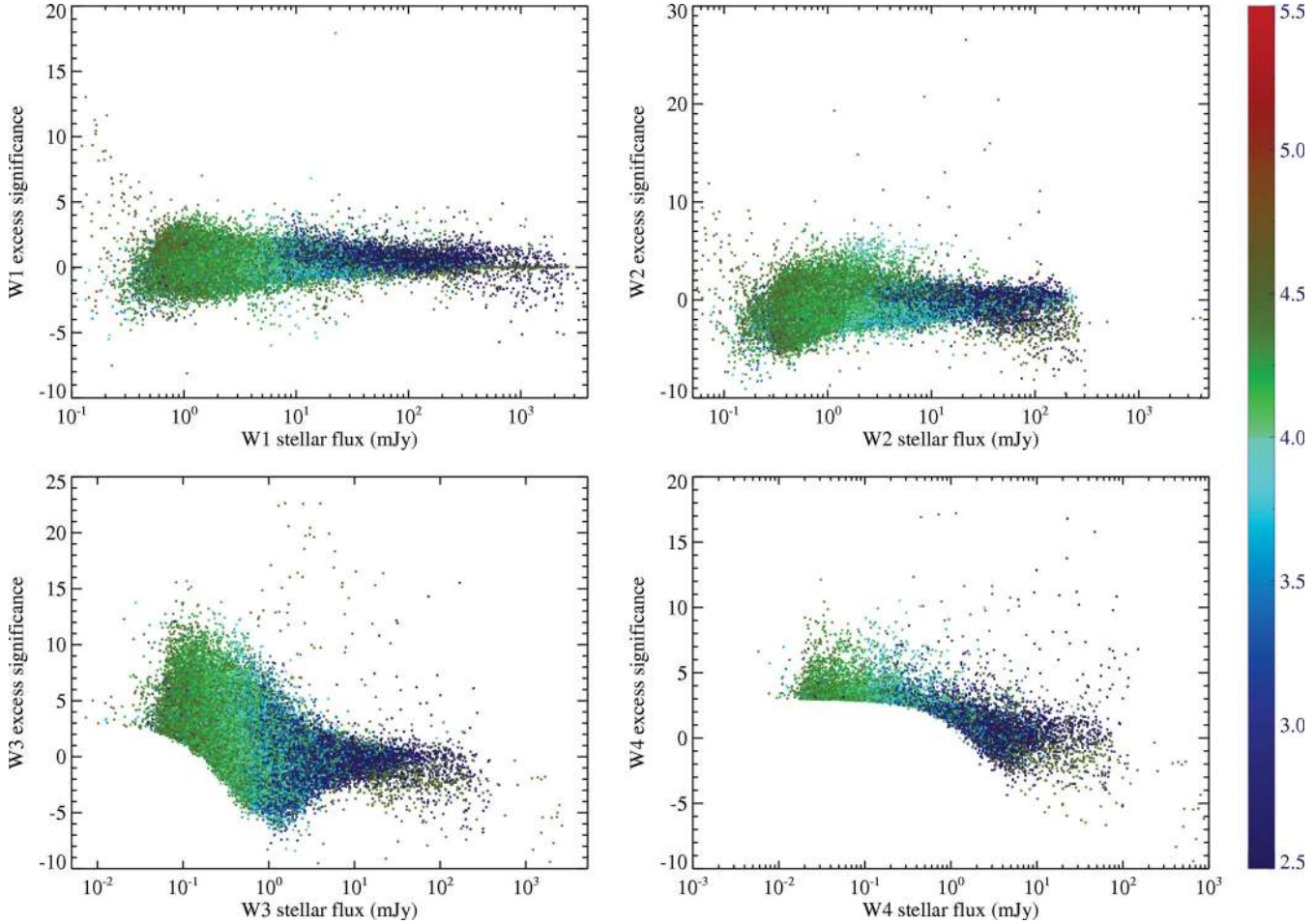

Figure 6. Excess significance versus predicted photospheric flux in the *W1–4* bands. The colour scale is log *g*. Any object with significance greater than 3–4 plausibly has a real excess.

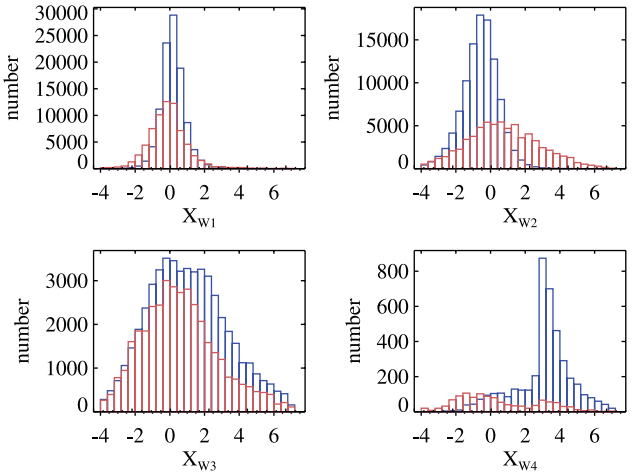

Figure 7. Excess significance histograms for the *W1–4* bands for stars hotter (filled bars) and cooler (empty bars, number multiplied by 15, 15, 10 and 1, respectively) than 4400 K.

Normally, this level would be around 3–4 if the uncertainties are estimated appropriately, but there are a very large number of *W3* excesses above this level. Fig. 7 shows the significance distributions, and *W3* clearly has many excesses that would be considered significant (as does *W4*, but to a lesser degree). These cannot be debris discs, because the excesses that *WISE* can detect around *Kepler* stars are rare. The distribution should therefore appear largely Gaussian with a dispersion of unity, with only a few objects at higher positive significance. Aside from being affected by sensitivity limits as seen for *W3–4*, the negative side of the histogram should be Gaussian (i.e. negative excesses cannot arise, even if positive excesses arise due to true astrophysical phenomena), and the extent can be used to estimate a reasonable significance threshold. Because the histograms do not show negative excesses below a significance of −4, we set the threshold at +4 for *W1–4*, and address the origin of the large number of excesses below.

We make an exception to this threshold for *W2* excesses around cooler stars. The significance distribution for *W2* is much wider than for hotter stars and skewed to larger values (Fig. 7). This difference presumably arises due to greater absorption in the *W2* band (see Section 3.1.2). Plotting the significance against metallicity indeed shows a strong correlation, which could be a sign that either *W2* excesses around M stars are strongly correlated with metallicity or the metallicity of these stars in the KIC is too high (i.e. the absorption in the model is stronger than in reality). Given that debris discs around nearby M dwarfs appear to be very rare (Lestrade et al. 2006, 2009; Gautier et al. 2007) and show no such trend, the latter is the more sensible conclusion and we set the significance threshold at 7.

4 INTERPRETATION OF EXCESSES

With our chosen significance criteria, there are 7965 disc candidates. There are 79, 95, 7480 and 1093 excesses in bands *W1–4*, respectively. These excesses correspond to an occurrence rate of about 4 per cent. Since about 4 per cent of nearby Sun-like stars have 24 μm excesses (e.g. Trilling et al. 2008) from calibration limited observations (flux ratios $\gtrsim$1.05), the finding of a similar rate from much less sensitive *WISE* observations (see Fig. 2) indicates that unless the stars observed by *Kepler* are somehow unique, most of the excesses cannot be due to debris. We therefore take a closer look at the origins of these excesses in the next two subsections. In what follows, we group stars into three effective temperature bins; 'M-type' ($T_{\rm eff} < 4400$ K), 'FGK-type' or 'Sun-like' ($4400 < T_{\rm eff} < 7000$ K), and 'A-type' ($7000 < T_{\rm eff} < 10\,000$ K). Only 10 excesses are found for stars hotter than 10 000 K, all in *W3*, and none survives the following analysis.

4.1 *W1–2* excesses: poor photospheric predictions

A handful of targets show *W1–2* excesses, but Fig. 8 argues that they are probably not due to circumstellar debris. Plotting the flux ratios in the *W1* and *W2* bands shows that these quantities are correlated, with a slope of approximately unity. The excess can therefore be accounted for by shifting the stellar spectrum upwards.

Inspection shows that the objects with the largest ($\gtrsim$1.5) flux ratios in *W1–2* are the result of failed photospheric fits, where the optical photometry is at odds with the *WISE* photometry. In these cases the stellar temperature is generally below 4400 K, and were not cut due to the relaxed photospheric fit χ^2 for these objects. These objects typically have no temperature in the KIC, meaning that no reasonable fit could be found there either.

Some objects have smaller flux ratios in *W1–2* that are also significant, but these ratios remain well correlated. While some are still due to poor photospheric predictions, another explanation is that the *W1–2* photometry includes two stars. The excess flux in the *W1–2* bands could be caused by the emission from a cooler star that lies within the instrumental point spread functions (PSFs) of all photometry (and may or may not be associated with the *Kepler* star in question). It is also possible that the higher resolution 2MASS and optical photometry used to predict the photosphere measured flux from one of a pair of stars, while *WISE* measured flux from both. Such a situation can also lead to the identification of an excess where there is none.[8]

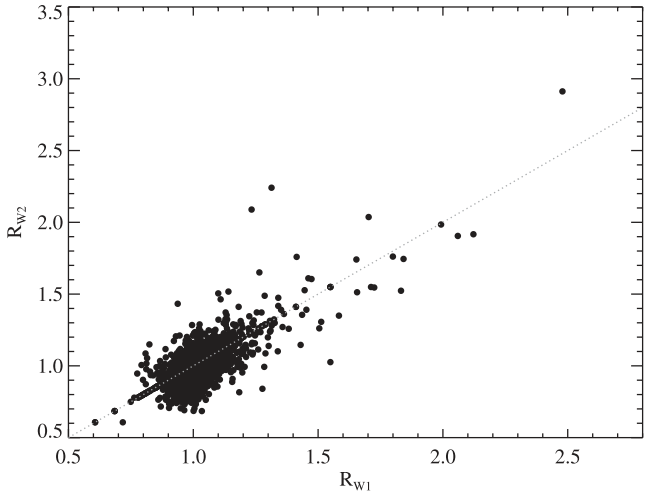

Figure 8. Flux ratios in the *W1* and *W2* bands compared for all stars with excesses (the dotted line is $y = x$, not a fit to the data). The strong correlation is not expected for dust emission and is largely due to poor photospheric predictions.

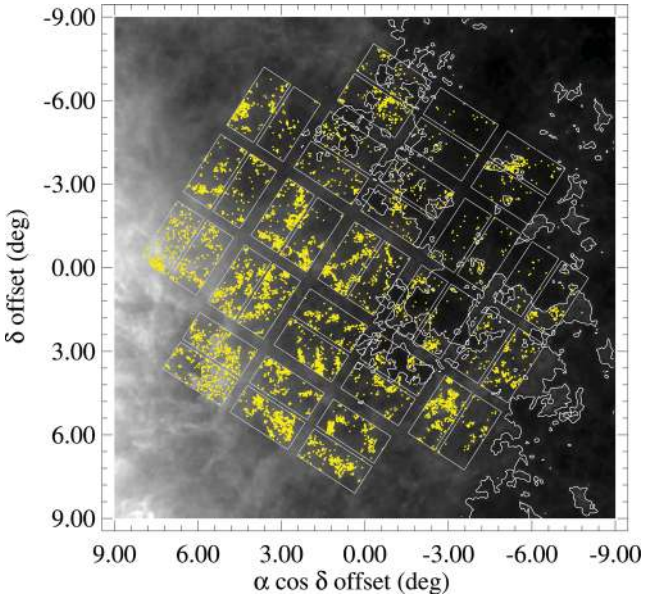

Figure 9. Clumping of stars with *W3* excesses (yellow dots) indicating that the excesses are due to the high background level. The 5 MJy sr^{-1} cut based on the *IRAS* 100 μm background image is shown by the white contours.

Based on the strong correlation between the flux ratios in *W1* and *W2*, we conclude that while some excesses are likely real in that the spectrum departs from our model of a single stellar photosphere, it is unlikely that any of the excesses are due to circumstellar dust.

4.2 *W3–4* excesses: discs or background?

While we have taken care to remove spurious detections (see Section 3.1.1), the *WISE* sensitivity and resolution and the very large sample size mean that extra-Galactic contamination due to chance alignments, even at very low levels, could contribute to, or even be the cause of, the *W3–4* excess population. Further, the low Galactic latitude of the *Kepler* field means that IR flux levels from dust within our Galaxy can be significant (see Fig. 1).

4.2.1 Galactic background contamination

The hypothesis that the Galactic background level is the cause of the very large number of *W3* excesses can be tested by simply plotting their locations on the sky, shown as dots in Fig. 9. The excesses clearly reside in clumps, and appear more frequent closer to the Galactic plane. Therefore, the bulk of the *W3* excesses are likely spurious.

To remove these false excesses in a way unbiased for or against the presence of excess emission therefore requires ignoring excesses in the highest background regions. Ideally this cut would be made

[8] An example is HIP 13642, identified by Koerner et al. (2010) as an excess because the MIPS observation includes two stars, while the 2MASS observation used to predict the photosphere resolves the pair.

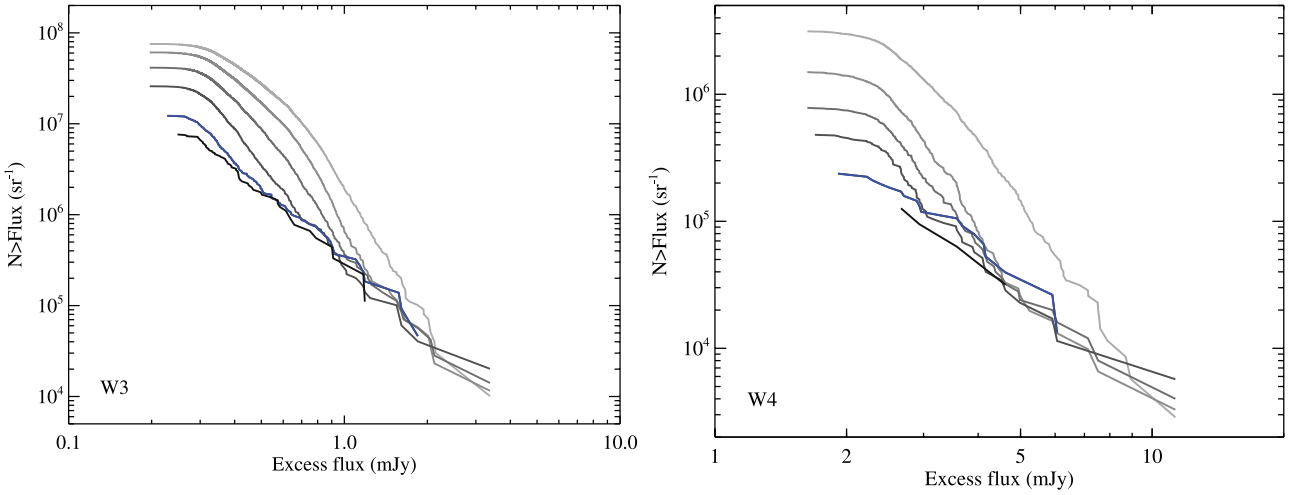

Figure 10. Cumulative source counts in *W3* (left-hand panel) and *W4* (right-hand panel). The solid lines show the counts for excesses as the cut in *IRAS* 100 μm background flux is increased. The lines show no cut (top line), and then levels of 15, 10, 7, 5 and 4 MJy sr^{-1}. As the cut in *IRAS* background decreases the excess counts approach a fixed level, indicating that the remaining excesses are not caused by Galactic background emission. The blue line shows our adopted cut level of 5 MJy sr^{-1}.

based on the *WISE* catalogue itself. In general, however, the background (`w3sky` column in the catalogue) is smooth, and shows no relation to the clumpiness seen for excesses except very near to the Galactic plane. This smoothness is perhaps a result of the dynamic *WISE* calibration, which attempts to remove temporal instrumental variations.[9] We found that instead the 100 μm *IRAS* IRIS map is a very good indicator of the background level, which we use to exclude sources below.

Fig. 10 shows how the cumulative number of excesses changes as a function of the *IRAS* background level. To make the plots comparable with those below, we scale the number of excesses by dividing by the area covered by the *WISE* observations. We take the observed area for a single star to be that enclosed by a circle whose diameter is the *WISE* PSF FWHM (6.5 and 12 arcsec for *W3–4*, respectively). These areas are multiplied by the number of non-giant stars with satisfactory SED fits that were observed and lie in regions below the given background level (and for which photometry was not removed for any of the reasons in Section 3.1.1).

In each plot the highest line shows the full set of excess counts. The lower lines show how the excess counts decrease as an increasing cut in the *IRAS* 100 μm background level is made. Once the cut level reaches about 5 MJy sr^{-1} the excess counts stop decreasing, indicating that the excesses that are due to the high background level have been removed. Higher cut levels do not decrease the distributions further and simply result in fewer remaining excesses.

The region where the *IRAS* background level is lower than 5 MJy sr^{-1} is shown in Fig. 9. The contours mark out and avoid regions where excesses clump together well. Based on this approach, we conclude that 5 MJy sr^{-1} is a reasonable cut level to avoid contamination from the high Galactic background level. Of the initial 7965 disc candidates, 271 remain after this cut.

4.2.2 *Extra-Galactic counts*

The remaining 271 excesses are generally real in the sense that they arise from point-like flux above the photospheric emission at the location of the *Kepler* stars. However, we now test whether these could arise from chance alignments with background galaxies. To estimate the number of excesses expected from extra-Galactic contamination we therefore first derive galaxy counts specific to our sample. The galaxy counts are derived by counting the number of sources above a given flux at a given wavelength after the contribution of Galactic stars has been removed.

Because galaxy counts may be subject to cosmic variance, and could appear to be different in the *Kepler* field due to stellar crowding and a relatively high background level near the Galactic plane, we show the results from several different fields and surveys in Fig. 11. For comparison with *WISE W3* we show 15 μm *ISO* results (La Franca et al. 2004) and for *W4* we show 24 μm *Spitzer* MIPS results (Papovich et al. 2004; Clements et al. 2011). We compare these with counts from two fields we extracted from the *WISE* catalogue. The first is a box in the *Kepler* field between 286°–296° right ascension and 40°–50° declination (71 deg^2). The second is a 'random' box farther away from the Galactic plane in Boötes, between 210°–220° right ascension and 30°–40° declination (82 deg^2, at a Galactic latitude of about 70°).

For our analysis of the *WISE* data we require A, B or C quality photometry (`ph_qual`), and S/N > 4, and remove the stellar contribution by keeping sources with *W1–W3, 4* > 1.2 (see Jarrett et al. 2011). These source counts are shown in Fig. 11 in grey, and follow the *ISO* and *Spitzer* counts well. The agreement suggests that cosmic variance is not significant for these fields (i.e. the distribution of background galaxies is similar in the *Kepler* field to elsewhere). The *WISE* counts are similar for both fields, though the *Kepler* field shows somewhat increased counts at the lowest flux levels.

We then add the cuts outlined in Section 3.1.1, which were made with the intention of minimizing galaxy contamination, for which the results are shown as black lines. The black lines lie below the grey ones, indicating that the extra cuts do indeed remove some galaxies. The cuts are more effective in *W4* with an overall decrease, while at *W3* the cuts are only effective for brighter galaxies. Because we want to quantify the extra-Galactic contribution to our excesses, we use the black line from the *Kepler* field as the expected level of galaxy contamination.

[9] http://wise2.ipac.caltech.edu/docs/release/allsky/expsup/sec4_4a.html

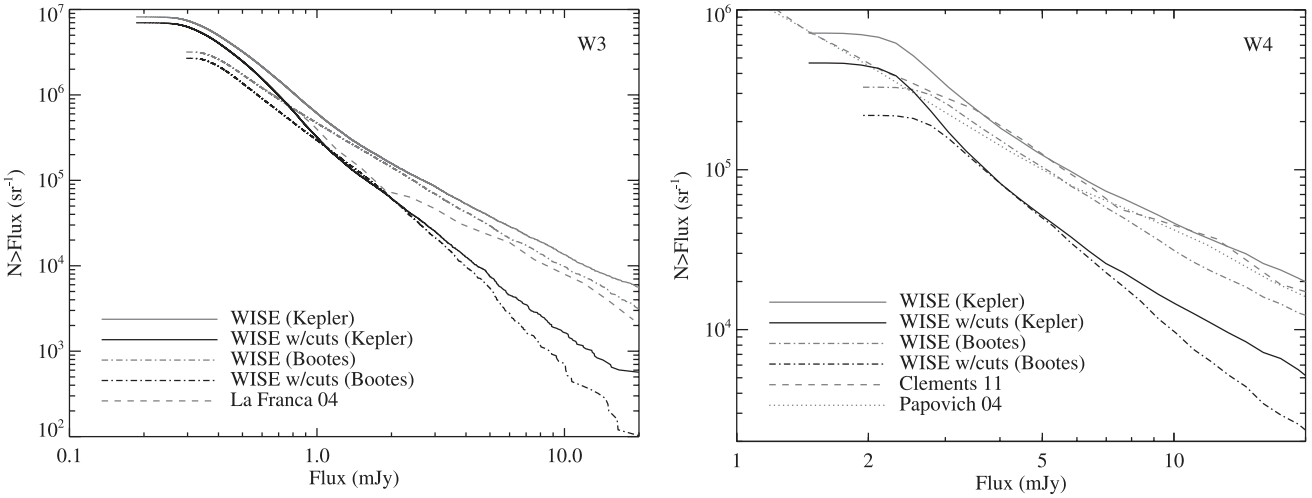

Figure 11. Comparison of cumulative galaxy source counts in *W3* (left-hand panel) and *W4* (right-hand panel). The grey lines show galaxy counts from *ISO* at 15 μm (left-hand panel; La Franca et al. 2004) and *Spitzer* MIPS at 24 μm (right-hand panel; Papovich et al. 2004), and from *WISE* in two different fields (see text). The black lines show the same *WISE* fields, but with the additional cuts outlined in Section 3.1.1 (i.e. the same cuts as were applied in our search for excesses around *Kepler* stars).

Table 1. The 271 *Kepler* stars with *WISE* 3–4 excesses. Columns are: KIC identifier, predicted *Kepler* (K_p) magnitude from the KIC, quarters the star was observed in (up to 6), fitted effective temperature, *W3–4* flux ratio and excess significance (where $X_{W3,4} \geq 4$). The 'Notes' column notes the single KOI, and potential planet hosts from Tenenbaum et al. (2012) ('T12'). This is a sample of the full table, which is available as Supporting Information with the online version of the article.

KIC	K_p	Quarters	T_{eff}	R_{W3}	X_{W3}	R_{W4}	X_{W4}	Notes
5866211	15.19	456	6585	4.2	5.0			
5866341	15.06	123456	6296	4.9	6.7			
5866415	15.33	123	6029	4.7	4.4			
6198278	14.86	123456	5436	2.8	4.1			
6346886	14.96	12346	5869	3.9	4.6			
6431431	14.87	123456	8147	5.9	7.8			
6503763	15.78	12346	5275	4.3	4.1			
6515382	13.29	123456	6265	1.7	4.2			
6516101	13.88	123456	6062	2.3	6.1			
6599949	15.42	123456	5773	4.0	4.1			
6676683	14.58	123456	6356	4.1	6.2			
6685526	15.00	123456	5103	2.7	4.1			KOI 861,T12

4.2.3 Extra-Galactic contamination

We now proceed with the remaining excesses where the *IRAS* 100 μm background is lower than 5 MJy sr^{-1} (listed in Table 1). The comparison of these excesses (again expressed as counts per sky area) and the galaxy counts derived above is shown in Fig. 12, where we have now separated the excesses by spectral type. In these plots, the galaxy counts do not move. The excess counts from discs depend on their occurrence rate and the distance to the stellar sample. Naturally, a higher disc fraction would move the excess counts upwards on this plot, away from the galaxy counts, and the chance of an individual excess being due to a background galaxy would be lower. For a fixed excess distribution, samples of stars that are on average fainter and brighter (i.e. farther and nearer) move the excess count lines left and right, respectively. Thus, the excess counts from discs for samples of brighter stars lie higher above the galaxy counts than samples of fainter stars, and again the likelihood of contamination is lower. This advantage arises because for fixed disc to star flux ratio (i.e. fixed disc properties), the absolute flux from a debris disc around a bright star is more than that from a faint star. At brighter flux levels the number of galaxies per unit sky area is smaller, so the likelihood of confusion lower. Finally, higher instrument resolution means less chance of confusion with a background galaxy because the area surveyed per star is smaller. Therefore, the same population of excesses observed with a larger telescope would also be further above the galaxy counts and more robust to confusion.

In Fig. 12, we make one additional cut to the number of stars that count towards the total area observed, by only including stars whose photospheres are equal to or brighter than that of the faintest star found to have an excesses. This photospheric flux cut makes use of the fact noted above that brighter stars are more robust to confusion (assuming that the presence or otherwise of a disc is independent of stellar brightness for fixed spectral type). This cut has little effect for most excesses because the faintest star with an excess is near the limit for all stars. However, it is effective for the *W4* excess associated with an A-type star because this star is brighter than the bulk of the sample. In *W3* the total number of non-giant stars that survive the cut in background level is 1198, 24916 and 1462 for M-type, FGK-type and A-type stars, respectively. In *W4* the

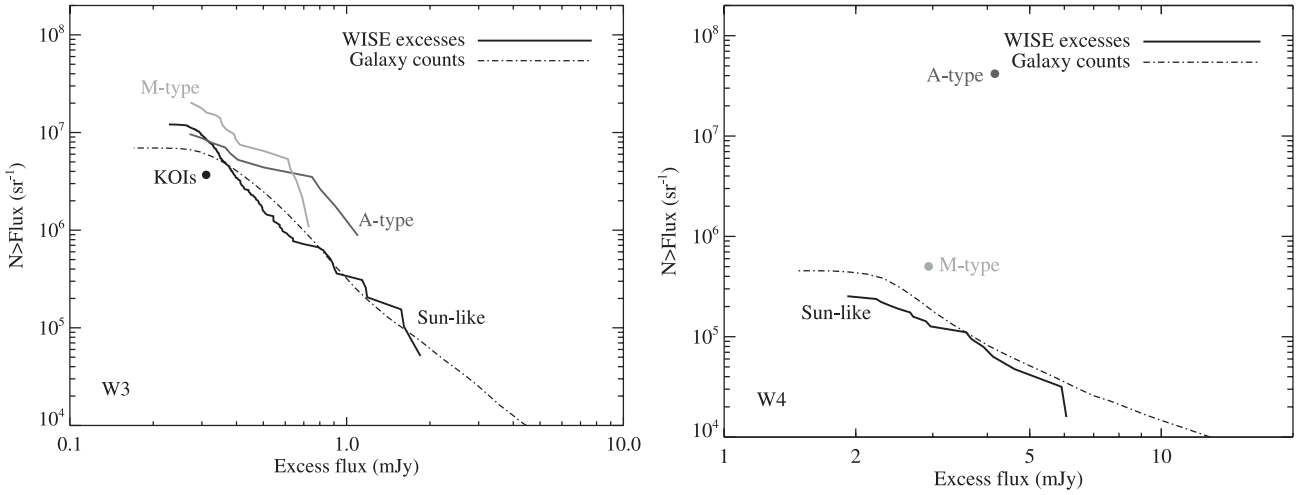

Figure 12. Cumulative source counts in *W3* (left-hand panel) and *W4* (right-hand panel). The solid lines show the counts for excesses, split into M-type, Sun-like and A-type (there are no *W4* excesses around M-types). The dot–dashed line shows our *WISE* counts in the *Kepler* field (solid lines in Fig. 11). The dot is the single planet host candidate found to have an excess (KOI 861). All excesses lie near the level expected from background galaxies, with the exception of a single *W4* excess around a nearby A-type stars.

numbers are 750, 23 742 and 10 for M, FGK and A-types. The very small number of A-type stars as bright or brighter than the one with an excess shows why the cut in photospheric flux is useful.

For *W3* (left-hand panel of Fig. 12), the excess counts for 19 M-type, 235 Sun-like and 11 A-type stars lie very close to the counts expected from background galaxies. Thus, not many, if any, of the excesses appear attributable to debris disc emission. The disc occurrence rate is insufficient to allow detection of debris discs that are robust to galaxy confusion (e.g. have a less than 1/10 chance of being a galaxy). The single *Kepler* planet host candidate (*Kepler* Object of Interest, or KOI) found to have an excess ((KOI 861 a.k.a. KIC 6685526; Borucki et al. 2011; Batalha et al. 2012) is shown as a single point, as one of 348 KOIs that survive the *IRAS* background cut. It lies very close to the A, FGK and M-type sample counts, so is equally likely to be confused. Because the excesses are heavily contaminated, the excess distributions represent an upper limit on the distribution of *W3* excesses that are due to debris discs (we return to these limits in Sections 5.3 and 6.).

For *W4* (right-hand panel of Fig. 12), the 16 Sun-like excess counts lie slightly below the galaxy counts, the single M-type excess slightly above, while the single A-type excess lies well above. Because galaxy counts are independent of stellar spectral type, there should be no difference between the contamination level for M-type, Sun-like and A-type stars. Therefore, the 22 μm A-type excess, which has a moderate 22 μm flux ratio of 1.63, is very likely due to debris disc emission. Because the difference between the A-type excess counts and the *WISE* galaxy counts is about a factor of 100, there is about a 1/100 chance that this A-star excess is a galaxy. It is likely that all Sun-like *W4* excesses and the single M-type excess can be explained as galaxy confusion, so again the disc occurrence rate is too low to allow robust disc detection and the excess counts represent an upper limit.

It is perhaps surprising that the excess and galaxy counts in Fig. 12 agree as well as they do. The galaxy counts were derived from all sources that met certain criteria within a specific patch of sky with the assumption that confusion only happens within the *WISE* PSF FWHM, while the excess counts were the result of the SED fitting method using *WISE* photometry at positions of known stars. We applied a cut in the background level to remove spurious excesses, but no such cut was required for the galaxy counts. The extra-Galactic counts in the *Kepler* field agree well with those for the Boötes field, where the *IRAS* 100 μm background level never reaches more than about 3 MJy sr^{-1} (i.e. is always below our cut in background level), so the extra-Galactic counts in the *Kepler* field are relatively unaffected by the background. Therefore, there appears to be a preference for stars (which are almost always detected in *W1–2*) to show a spurious *W3–4* flux due to high background levels, while galaxies (which are generally not detected in *W1–2*) do not. This difference may be attributed to the *WISE* method of source extraction, which attempts to measure fluxes across all four bands if a source is detected in at least one.

4.3 Comparison with previous results

Our study is not the first to use *WISE* to look for warm emission from discs around *Kepler* stars (Lawler & Gladman 2012; Ribas et al. 2012). In a similar study, Krivov et al. (2011) reported two disc candidates in the *WISE* preliminary release catalogue from a sample of 52 stars known to host transiting planets [one of the candidate systems was TrES-2 a.k.a. KOI 1, the first transiting planet host found in the *Kepler* field (O'Donovan et al. 2006)]. These two systems were called into question by Ribas et al. (2012) after inspection of the images, and become upper limits on any disc emission in the all-sky release (A. Krivov, private communication).

Ribas et al. (2012) found 13 candidate disc systems using the *WISE* preliminary release, 12 of which are observed by *Kepler* (the other is WASP-46, a nearby system with a transiting planet; Anderson et al. 2012). However, they use an excess significance threshold of 2 (see equation 3). At this level 2.3 per cent of systems are expected to have significant excesses purely due to the fact that the uncertainties have a distribution (that is assumed to be Gaussian). Therefore, of the 468 *Kepler* planet host candidates they considered, 11 should lie above this threshold. This number is similar to their 12 disc candidates, so these candidates are consistent with being part of the expected significance distribution if no stars have discs.

Three of their 12 disc candidates have significance higher than 3, but all lie in regions where the 100 μm background is higher than

5 MJy sr^{-1} so are excluded from our analysis because their excesses are likely due to the high background level (Section 4.2.1).[10]

In contrast to our conclusions, Ribas et al. (2012) find that background contamination is negligible, with a 5×10^{-5} chance of a galaxy brighter than 5 mJy appearing within 10 arcsec of a source at 24 μm, using counts from Papovich et al. (2004). However, these counts show about 10^5 sr^{-1} for sources brighter than 5 mJy (see Fig. 11), so a target area of 314 arcsec^2 (10 arcsec radius) yields $10^5 \times 314 \times 2.35 \times 10^{-11} = 0.001$ probability of having a 5 mJy background source within 10 arcsec of a target. However, the *WISE* beam is in fact smaller than 10 arcsec radius, so using 6 arcsec is more appropriate (see the previous subsection). Furthermore, removing *WISE* photometry that is flagged as extended decreases the *W4* counts (Fig. 11), so the Papovich et al. (2004) counts overestimate the confusion level that applies here by a factor of about 2. Therefore, 0.06 spurious excesses are expected from 468 targets. This expectation is in line with the two sources they report with *W4* excesses, KIC 2853093 and KIC 6665695, since these have *W4* S/N of 2.2 and 2.5, respectively, and as noted above we would not consider these significant given the sample size.

All of their candidates have 12 μm excesses, so should be compared with galaxy counts at a similar wavelength (e.g. 15 μm *ISO* counts). Based on Fig. 11, about 5×10^6 background galaxies per steradian are expected down to the detection limit of about 3 mJy, which for a target radius of 3.25 arcsec (33 arcsec^2) yields an expected contamination rate of $5 \times 10^6 \times 33 \times 2.35 \times 10^{-11} = 0.004$. Thus, about two spurious excesses among 468 targets are expected at this wavelength. Of their *W3* disc candidates, three have excesses more than 3σ significant. However, KOI 1099 has *W3–4* upper limits in the newer all-sky release, so the expectation of two spurious excesses appears to be met. Both sources lie in the regions we excluded due to the high background so the *WISE* photometry may still be spurious.

In a similar study, Lawler & Gladman (2012) reported the discovery of excess emission around eight *Kepler* planet-host stars using the *WISE* preliminary release. They used a significance criterion of 5σ, so their excesses should be astrophysical (i.e. not statistical). There are only three candidates in common with Ribas et al. (2012). However, these are the three noted above with a significance greater than 3σ, so Lawler & Gladman (2012) find the same candidates as Ribas et al. (2012) with an additional five disc candidates. Of their eight, the *WISE W3* and *W4* measurements of KOI 904 and KOI 1099 are upper limits in the newer all-sky *WISE* catalogue, and KOIs 871, 943, 1020 and 1564 were rejected by Ribas et al. (2012) after image inspection. The same two plausible disc candidates remain, so the number is again consistent with the number expected from confusion. Though the details vary, these two studies are basically consistent if a 3–5σ significance criterion is used and candidates are rejected based on the images.

4.4 Debris disc candidate

We now briefly outline some properties of our most promising disc candidate, KIC 7345479 (with a *Kepler* K_p magnitude of 7.9), shown in Fig. 13. Assuming that this star is a dwarf yields a distance of 280 pc, much closer than most *Kepler* stars. The SED shows the 9700 K stellar spectrum, along with a simple blackbody fit to the excess that includes the *W2–4* photometry. With a measured flux of 10.8 ± 0.9 mJy and a photospheric flux of 6.6 ± 0.2 mJy the *W4* excess has a flux ratio $R_{W4} = 1.6$, with significance $X_{W4} = 4.5$. The disc temperature is constrained by the *W3* upper limit, so is cooler than about 200 K, corresponding to a radial distance of greater than 15 au and lies beyond the region of *Kepler* sensitivity to transiting planets. The fractional luminosity for the blackbody model shown is 3.25×10^{-5}. As we show in Section 5, aside from the potential for planet discovery around the host star, this disc is fairly unremarkable within the context of what is known about discs around nearby A-stars.

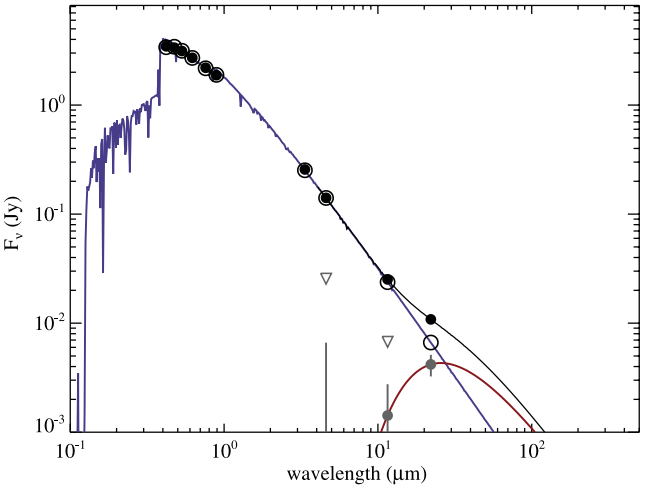

Figure 13. SED for the A-type *W4* debris disc candidate KIC 7345479. The stellar spectrum is shown in blue, and the fitted blackbody in red. The sum of the two is shown in black. KIC and *WISE* photometry is shown as black dots, and synthetic photometry of the star in the same bands as open circles. Grey symbols show the star-subtracted fluxes, with a triangle above indicating the 4σ upper limit if necessary.

5 NEARBY STAR COMPARISON

There should be nothing particularly special about *Kepler* stars compared to nearby stars, so we compare our survey with 24 μm results from two large unbiased *Spitzer* surveys of nearby stars. Because the results can only be interpreted within the context of what was possible with each survey, we first compare the sensitivity to discs for the *Spitzer* surveys in the fractional luminosity versus temperature space introduced in Fig. 2. We also make a brief comparison with *IRAS* results at 12 μm.

5.1 Disc sensitivity at 22–24 μm

The left-hand panels of Fig. 14 show the sensitivity to discs with *WISE* at 22 μm, split into Sun-like and A-type stars. The plots are similar to Fig. 2, but now represent the cumulative sensitivity for all objects. Discs in the white region could have been detected around all stars, and discs in the black region could not have been detected around any star.

For the Sun-like *Kepler* stars observed with *WISE* (top left panel), the region covered for the bulk of the stars is similar to that predicted in Fig. 2. Only the brightest few stars have sensitivity to fractional luminosities lower than about 0.1 per cent. No discs are shown

[10] KOI 469 has a very bright moving object (i.e. an asteroid or comet) visible in the *WISE* images at a separation of about 6 arcmin, which may have affected the source extraction. Given the rarity of excesses, it seems more likely that the apparent excess is due to the presence of the bright object, rather than coincidental.

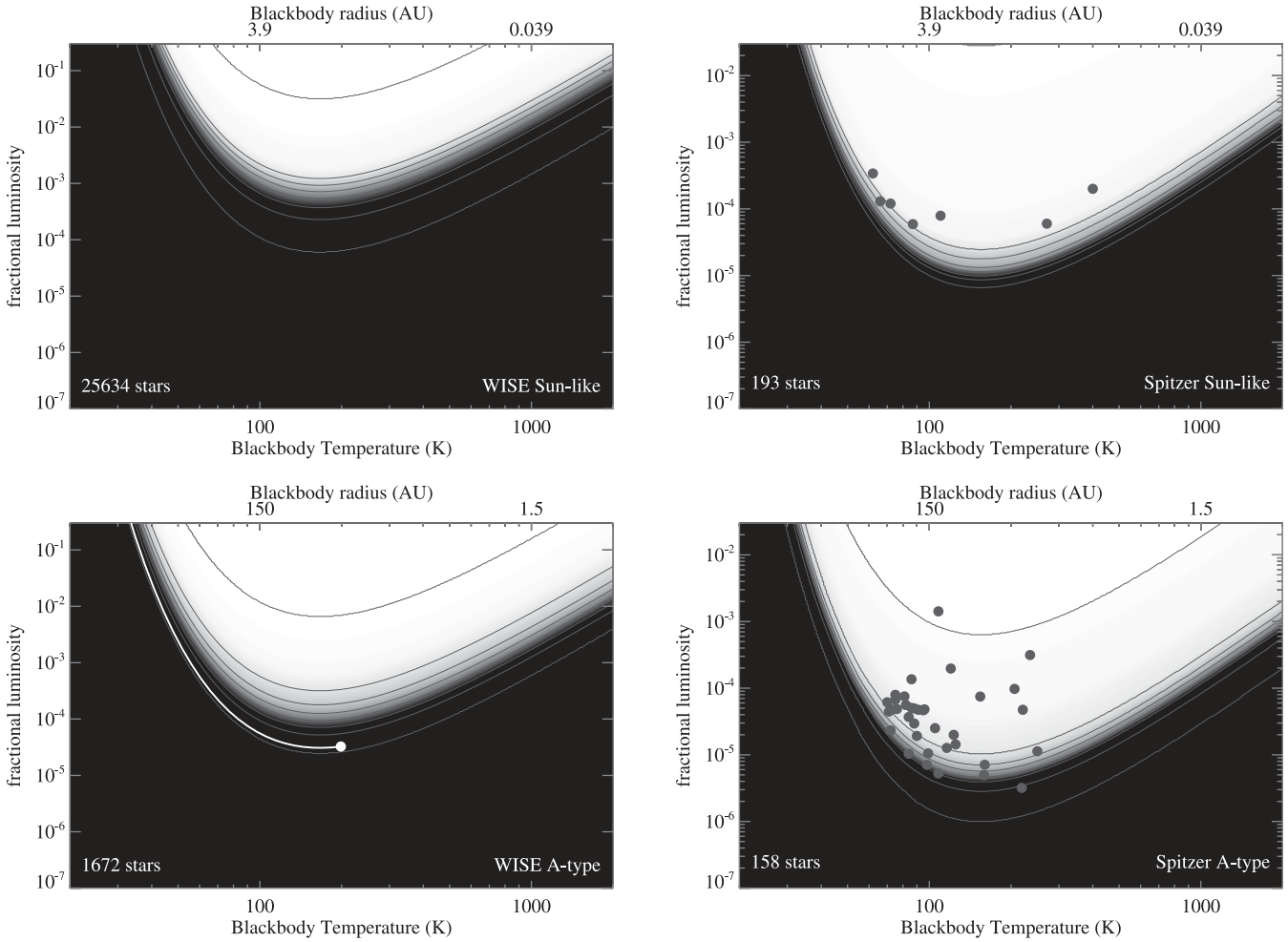

Figure 14. Sun-like (top row) and A-type (bottom row) disc sensitivity comparison between *WISE* 22 μm (left-hand column) and nearby stars with *Spitzer* MIPS at 24 μm (right-hand column). Discs in regions of the parameter space that are white could be detected around all stars, and discs in black regions could not be detected around any star. The colour scale is a linear stretch; contours show eight linearly spaced levels from one to the number of stars observed in each case. The top radial scale assumes $L_\star = 0.5\,L_\odot$ for Sun-like stars and $L_\star = 20\,L_\odot$ for A-types. The A-star disc candidate is shown at the temperature fitted in Fig. 13, but could lie anywhere along the white line because the temperature is only an approximate upper limit.

on this plot because the *W4* excesses around Sun-like stars are consistent with arising entirely from background galaxies.

The *WISE* sensitivity is in contrast to that for nearby Sun-like stars observed with *Spitzer* at 24 μm (top right panel; Trilling et al. 2008), which could detect discs with much lower fractional luminosities (i.e. the white region extends to lower f). The *WISE* sensitivity does not extend into the region where discs were detected with *Spitzer*, so does not probe the same part of the disc distribution as the *Spitzer* study.

Compared to nearby A-stars observed with *Spitzer* (lower-right panel), the disc and lowest contours for *WISE* extend into the region covered by the brightest excesses found by Su et al. (2006) (i.e. where $T_{\rm disc} \sim 100$–200 K and $f \sim 10^{-3}$ to 10^{-4}). Unlike the Sun-like stars, there is therefore some overlap in the parts of the disc distributions that are detectable with each survey. For the *WISE* A-star disc candidate (dot in lower-left panel) we assume the disc properties shown in Fig. 13. Because this temperature is an approximate upper limit, the disc could lie anywhere along the white line that curves towards the upper left of the figure (though cooler discs must have significantly higher fractional luminosities). The *WISE* detection is very likely typical based on where it lies relative to the known distribution of A-star excesses.

5.2 Excess distribution at 22–24 μm

Fig. 15 shows cumulative 22 and 24 μm flux ratio distributions, again split into Sun-like and A-type samples. The nearby star distributions are simply the cumulative distribution of flux ratios, since all observed stars were detected.

For Sun-like stars (left-hand panel), because we concluded that all *W4* Sun-like excesses were consistent with arising from contamination by background galaxies (Section 4.2, Fig. 12), the *WISE* part of the distribution is an upper limit on the occurrence rate of rare bright discs. It is found by assuming upper limits on flux ratios are detections (i.e. by assuming that all stars could have discs just below detectable levels, whereas the true distribution lies somewhere below this level). The lack of overlap in the distributions due to the rarity of large 22–24 μm excesses, and the limitations of *WISE* observations of *Kepler* stars, is clear.

While lower levels of excess (flux ratios of ∼1.1–2) have an occurrence rate of around 2–4 per cent around Sun-like stars (e.g. Fig. 15, Hines et al. 2006; Beichman et al. 2006b), large ($\gtrsim$2) excesses were previously constrained to less than about 0.5 per cent based on the Trilling et al. (2008) sample. We have set new limits 1–2 orders of magnitude lower and, as the left-hand

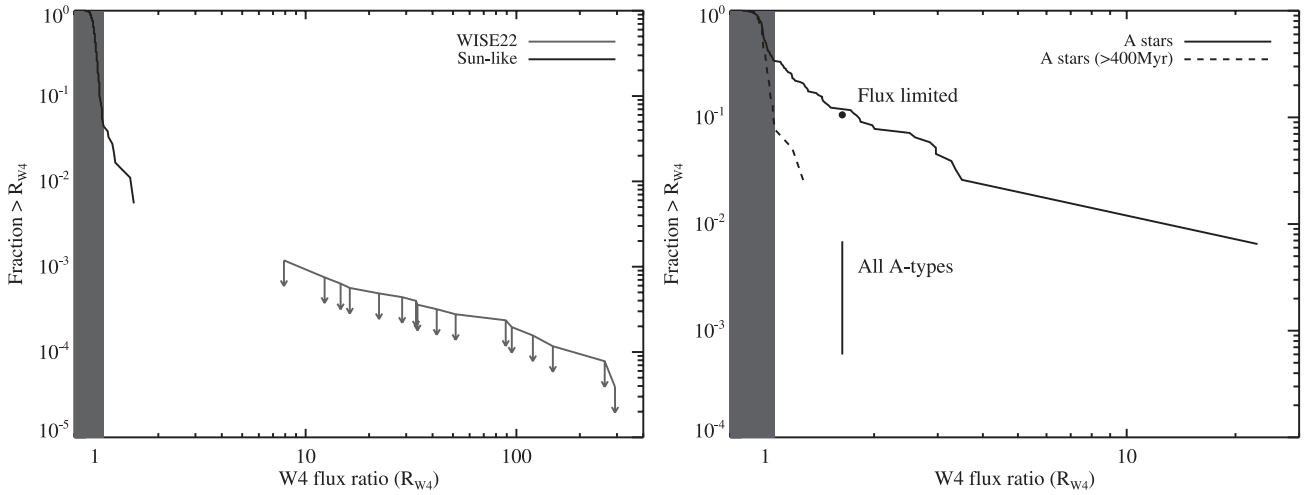

Figure 15. Comparison of 22 and 24 μm flux ratio distributions for *WISE* and nearby stars (Su et al. 2006; Trilling et al. 2008). The left-hand panel shows Sun-like stars, for which the *WISE* distribution is an upper limit. The right-hand panel shows A-type stars, and the *WISE* points are based on the full and flux limited samples and the single disc candidate (see text). We also show a distribution for nearby A-stars older than 400 Myr. The dark regions mark where the *Spitzer* observations were calibration limited, below 1.1 (left, Trilling et al. 2008) and below 1.06 (right, Su et al. 2006).

panel of Fig. 15 shows, these limits apply to large flux ratios of 10–300.

For the A-type stars (right-hand panel), we show the excess occurrence rate for the single A-star with a *W4* excess of 1.63. Of the nine stars in the photospheric flux limited sample without an excess (stars as bright or brighter than the one with an excess), one has an upper limit higher than 1.63, while the others are lower (i.e. the observations could have detected a disc like the one found). The occurrence rate at this flux level therefore lies between 1/9 and 1/10, with these extremes set by assuming that the highest upper limit is either a detection above 1.63 or unity (a non-detection below 1.63). This point is shown as 'flux limited' on Fig. 15, and is consistent with the sample of Su et al. (2006). With only a single detection this occurrence rate is of course very uncertain.

Using the full sample of our A-stars yields a lower disc occurrence rate, with at least 145 stars for which this flux ratio could have been detected. If all upper limits are assumed to be non-detections below 1.63 then the occurrence is one from 1672 stars. The vertical line in Fig. 15 shows the range set by these two limits, which lies below the point set from the photospheric flux limited sample, and below the distribution of nearby A-stars.

While these two occurrence rates are very uncertain due to only a single disc detection, we consider some possible reasons for the discrepancy. One possibility is an age bias, as most stars in Su et al. (2006) were chosen based on cluster or moving group membership and are therefore younger on average than field A-stars. Cutting the nearby A-star sample to only contain stars older than 400 Myr shows that a difference in sample ages has a significant effect on the flux ratio distribution (i.e. discs evolve with time, Rieke et al. 2005; Siegler et al. 2007). Though the extrapolation of the >400 Myr population is very uncertain, this older subsample is more consistent with the *WISE* excesses from the full sample. The difference in the distributions could therefore be understood if A-stars in the *Kepler* field are typically older than about 400 Myr. While there should be no such bias for stars of the same spectral type, there is in fact a difference in the typical spectral types between the *Spitzer* A-star survey and those observed with *WISE*. While the *Spitzer* sample comprises late B and early A-types, our *Kepler* A-stars are mostly at the lower end of the 7000–10 000 K temperature range (i.e. are late A and early F-types). Later spectral types both have lower disc occurrence rates and are typically older due to longer main-sequence lifetimes (e.g. Siegler et al. 2007), which could account for the lower detection rate. It is therefore the higher detection rate inferred from the single *WISE* excess (around a 9700 K star) that may be odd, but given the small number (i.e. one disc from 10 stars) can be attributed to chance and that the star with an excess is hotter than most.

5.3 Excess distribution at 12 μm

We have also set stringent limits on the distribution of warm discs at 12 μm. At 12 μm, previous knowledge of the excess distribution was derived from the all-sky *IRAS* survey (e.g. Aumann & Probst 1991). While many authors have used the results of this survey to discover and study warm excesses (e.g. Song et al. 2005; Chen et al. 2006; Moór et al. 2009; Smith & Wyatt 2010), few have published the results from an unbiased sample at this wavelength in a manner that allows the distribution of the 12 μm flux ratios to be determined. Fig. 16 shows our upper limit on the 12 μm flux ratio distribution for Sun-like stars, showing that bright excesses at this wavelength are extremely rare. For comparison, we show the lack of excess detection among 71 FGK stars detected at 12 μm (Aumann & Probst 1991), which was calibration limited and could not detect flux ratios smaller than 1.14. We also show the distribution of *IRAS* 12 μm flux ratios for 348 FGK stars in the Unbiased Nearby Star (UNS) sample (Phillips et al. 2010), based on photospheric modelling done for the *Herschel* DEBRIS survey (e.g. Matthews et al. 2010; Kennedy et al. 2012), which has a similar flux ratio sensitivity. The only significant excess is for η Corvi (HD 69830 is the second largest excess, but with a flux ratio of 1.13 is only about 2σ significant).[11] These constraints and detections are all consistent, and set limits on the rarity of bright 12 μm excesses to less than one in every thousand to ten thousand stars for flux ratios greater than about 5.

[11] Several other stars in this sample show significant excesses, but these can be shown to be spurious based on more recent *Spitzer* MIPS and *Herschel* PACS observations that resolve the star and a nearby background source.

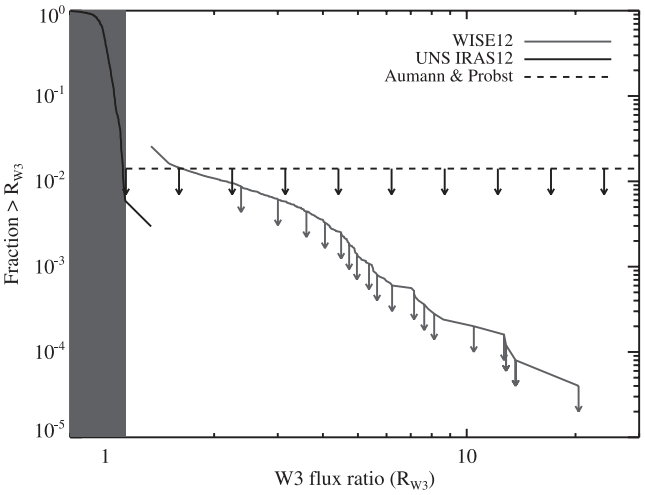

Figure 16. Upper limits on the 12 μm flux ratio distribution from *IRAS* (dashed line) and *WISE* (solid grey line), compared to the distribution for stars in the UNS sample using *IRAS*. The dark region marks where the *IRAS* detections were calibration limited (below 1.14).

6 DISCUSSION

One of several goals of this study was to test for a correlation between the existence of debris discs and planets discovered by *Kepler*. However, the distribution of the rare bright excesses that *WISE* is sensitive to around *Kepler* stars was not known at the outset, so whether this goal was possible was not known either. We noted that even if bright discs were too rare among the bulk population a possible correlation between discs and low-mass planets may allow robust disc detections among this subset.

Only one *Kepler* planet candidate host (of 348 KOIs that were not excluded by the 100 μm background cut) was found to have an excess, so this possibility appears unlikely. In addition, Fig. 12 shows that this detection rate is close to that expected from galaxy confusion. Thus, for the bright warm excesses that *WISE* is sensitive to, there is no evidence that planet host candidates have a disc occurrence rate that is different from the bulk population.

Similarly, excesses around the remaining *Kepler* stars are also consistent with arising from chance alignments with background galaxies, with the exception of a single A-type star. However, the possibility that a small number of the excesses are true debris discs means that the chance of detecting transiting dust concentrations is at least as good as for *Kepler* stars without excesses, and may be higher (the 271 Kepler stars with *W3* or *W4* excesses are listed in Table 1). Discovery of many such dust transits that preferentially occur around stars with excesses would argue that at least some excesses are debris discs, though this verification method seems unlikely to succeed.

We have therefore set new limits on the distribution of warm excesses. The range of flux ratios for which we have set limits for Sun-like stars is 2–20 at 12 μm (Fig. 16) and 10–300 at 22 μm (left-hand panel of Fig. 15). For such large 12–22 μm excesses to arise from steady-state processes the planetesimal belts would have to be either around very young stars or relatively distant from their central star (Wyatt et al. 2007), which in turn requires fractional luminosities $\gtrsim$1 per cent (see Fig. 2). Detecting large warm excesses around main-sequence stars is very unlikely because collisional evolution depletes belts near the central star to undetectable levels rapidly, so the conclusion is that such mid-IR excesses are most likely transient. Two main processes seem to be plausible causes of such excesses. The first, delivery of material from an outer reservoir (Beichman et al. 2005; Wyatt et al. 2007), is appealing because short-lived warm dust can be replenished using material from a long-lived outer belt. Alternatively, because we are here interested in large excesses, the debris from a giant impact between large bodies is a possibility (i.e. perhaps similar to the Earth–Moon forming event; Jackson & Wyatt 2012).

Several possibilities exist for the delivery of objects from an outer belt to terrestrial regions. A system of sufficiently many planets on stable orbits can pass objects inwards from an outer belt (Bonsor & Wyatt 2012), or a planetary system instability can severely disturb a planetesimal population, some of which end up in the terrestrial zone (Gomes et al. 2005). Such possibilities have been suggested as mechanisms to generate the warm dust component observed around η Corvi (Booth et al. 2009; Lisse et al. 2012).

Because at least 15 per cent of Sun-like stars have cool outer planetesimal belts (e.g. Trilling et al. 2008), our limits of 0.01–0.1 per cent for warm belts (for the flux ratios noted above for 12 and 22 μm) mean that fewer than one in 150–1500 can be generating large levels of warm dust from cool outer belts at any given time. This fraction could in fact be larger because the 15 per cent only represents discs down to a particular detection limit, and cool discs too faint to detect could still have enough material to produce large warm dust levels (Wyatt et al. 2007). Booth et al. (2009) placed similar limits on the number of systems that could be caught in the act of an instability that delivers large amounts of debris to the terrestrial region, estimating that less than about 0.2 per cent (i.e. 1/500) of Sun-like stars might be observed undergoing an instability at 24 μm.

Whether such instabilities do produce very large excesses is another question. In studying the dust emission generated in their model of the Solar system's proposed planetary instability, Booth et al. (2009) find that while the relative changes can be very large, the flux ratios are near unity at 12 μm and of the order of 10 at 24 μm. However, these ratios may be underestimated because they do not include emission that could arise from the sublimation of comets within 1 au. It is therefore hard to say whether these results are representative, since they will also depend on the specific system architecture. The η Corvi system has been suggested as a possible candidate currently undergoing such an instability, and shows a 12 μm flux ratio of 1.3. If typical, these results suggest that instabilities may not produce the larger excesses considered here.

In contrast, the giant impact scenario can produce extremely large excesses (Jackson & Wyatt 2012). The relatively nearby star BD+20 307 (at 96 pc), which has a 10 μm flux ratio of about 100, is a good candidate for such an event (Song et al. 2005; Weinberger et al. 2011). While such events would generally be expected to be associated with young systems, where the final ∼10–100 Myr chaotic period of giant impacts and terrestrial planet formation are winding down (e.g. Chambers & Wetherill 1998; Chambers 2001), BD+20 307 is a $\gtrsim$Gyr old main-sequence binary (Zuckerman et al. 2008). The excess may therefore be indicative of a recent instability that has greatly increased the chance of collisions within the terrestrial zone, and is unrelated to planet formation (Zuckerman et al. 2008). Clearly, age estimates for the host stars are important for understanding the origin of dust in such systems.

While the *WISE* mission might appear to permit near-unlimited sample sizes to help detect the aftermath of the rarest collision events, we have shown that their detection among *Kepler* stars is fundamentally limited. This limit arises because the occurrence rate of excesses that can be detected is too low, so the discs are overwhelmed by galaxy contamination. Because *Kepler* stars represent

a sample that will remain unique for the foreseeable future, it is desirable to find ways to overcome this issue. Based on the findings of Section 4.2, one option is to create sub-samples that maximize the chance of disc detection, because higher disc occurrence rates are more robust to galaxy contamination. Younger stars tend to have larger excesses that are also more frequent (e.g. Rieke et al. 2005; Siegler et al. 2007; Carpenter et al. 2009), so a sub-sample of young stars will be more robust to confusion. The long-term monitoring of *Kepler* stars may provide some help if accurate stellar ages can be derived, for example if rotation periods can be derived to yield age estimates via gyrochronology (Skumanich 1972; Barnes 2007; Mamajek & Hillenbrand 2008). Another way to split the sample is by spectral type, because earlier-type stars are brighter and have higher disc occurrence rates (for fixed sensitivity). This approach is less appealing for studying the links between discs and planets, however, because the bulk of stars observed by *Kepler* are Sun-like.

If we allow for the possibility of observing *Kepler* stars with *WISE* excesses with other instruments, there is a potential gain with better resolution. A galaxy that is unresolved with *WISE* might be resolved with *Spitzer*'s Infrared Array Camera (IRAC) instrument, or using ground-based mid-IR observations on 8-m-class telescopes for example. Assuming that it could be detected, the high ($\sim$0.5 arcsec) resolution of such ground-based observations would have over a 99 per cent chance of detecting a galaxy that was not resolved with the *WISE* beam at 12 μm. Therefore, detection of fewer galaxies than expected in a sample of targets (e.g. significantly fewer than 99 out of 100) would be evidence that the excesses do not randomly lie within the *WISE* beam and that some are therefore due to excesses centred on the star (i.e. are debris discs).

Ultimately, we found that searching for debris discs around stars in the *Kepler* field with *WISE* is limited by the high background level and galaxy contamination. While high background regions can be avoided, background galaxies will always be an issue for such distant stars. Though it means being unable to study the planet–disc connection with such a large planet-host sample, nearby stars should be the focus of studies that aim to better define the distribution of warm excesses. Characterizing this distribution is very important, particularly for estimating the possible impact of terrestrial-zone dust on the search for extra-solar Earth analogues (e.g. Beichman et al. 2006a; Roberge et al. 2012). For example, extending the distribution to the faintest possible level available with photometry (calibration limited to a 3σ level of $\sim$5 per cent) yields a starting point to make predictions for instruments that aim to detect faint 'exozodi' with smaller levels of excess. Because bright warm debris discs must decay to (and be observable at) fainter levels, the distribution will also provide constraints on models that aim to explain the frequency and origin of warm dust.

7 SUMMARY

We have described our search of about 180 000 stars observed by *Kepler* for debris discs using the *WISE* catalogue. With the completion of the *AKARI* and *WISE* missions, such large studies will likely become common. We have identified and addressed some of the issues that will be encountered by future efforts, which mainly relate to keeping spurious excesses to a minimum by using information provided in photometric catalogues.

We used an SED fitting method to identify about 8000 IR excesses, most of which are in the 12 μm *W3* band around Sun-like stars. The bulk of these excesses arise due to the high mid-IR background level in the *Kepler* field and the way source extraction is done in generating the *WISE* catalogue. From comparing the number counts for excesses in low background regions with cosmological surveys and *WISE* photometry from the *Kepler* field, we concluded that a 22 μm excess around a single A-type star is robust to confusion, with about a 1/100 chance of arising due to a background galaxy. We found no evidence that the disc occurrence rate is any different for planet and non-planet host stars.

In looking for these discs we have set new limits on the occurrence rate of warm bright discs. This new characterization shows why discovery of rare warm debris discs around Sun-like *Kepler* stars in low background regions is generally limited by galaxy confusion. Though the planetary aspect would be lost, nearer stars should be the focus of future studies that aim to characterize the occurrence of warm excesses.

ACKNOWLEDGMENTS

We thank the reviewer for a thorough reading of this article and valuable comments. This work was supported by the European Union through ERC grant number 279973. This research has made use of the following: The NASA/ IPAC Infrared Science Archive, which is operated by the Jet Propulsion Laboratory, California Institute of Technology, under contract with the National Aeronautics and Space Administration. Data products from the *WISE*, which is a joint project of the University of California, Los Angeles, and the Jet Propulsion Laboratory/California Institute of Technology, funded by the National Aeronautics and Space Administration. Data products from the 2MASS, which is a joint project of the University of Massachusetts and the Infrared Processing and Analysis Center/California Institute of Technology, funded by the National Aeronautics and Space Administration and the National Science Foundation. The Multimission Archive at the Space Telescope Science Institute (MAST). STScI is operated by the Association of Universities for Research in Astronomy, Inc., under NASA contract NAS5-26555. Support for MAST for non-*Hubble Space Telescope* data is provided by the NASA Office of Space Science via grant NNX09AF08G and by other grants and contracts. Data collected by the Kepler mission. Funding for the Kepler mission is provided by the NASA Science Mission directorate. This work was supported by the European Union through ERC grant number 279973.

REFERENCES

Absil O. et al., 2006, A&A, 452, 237
Anderson D. R. et al., 2012, MNRAS, 422, 1988
Aumann H. H., Probst R. G., 1991, ApJ, 368, 264
Aumann H. H. et al., 1984, ApJ, 278, L23
Barnes S. A., 2007, ApJ, 669, 1167
Batalha N. M. et al., 2010, ApJ, 713, L109
Batalha N. M. et al., 2011, ApJ, 729, 27
Batalha N. M. et al., 2012, ApJS, submitted (arXiv:1202.5852)
Beichman C. A. et al., 2005, ApJ, 626, 1061
Beichman C. A. et al., 2006a, ApJ, 652, 1674
Beichman C. A. et al., 2006b, ApJ, 639, 1166
Beichman C. A. et al., 2011, ApJ, 743, 85
Bonsor A., Wyatt M. C., 2012, MNRAS, 420, 2990
Booth M., Wyatt M. C., Morbidelli A., Moro-Martín A., Levison H. F., 2009, MNRAS, 399, 385
Borucki W. J. et al., 2003, in Blades J. C., Siegmund O. H. W., eds, SPIE Conf. Ser. Vol. 4854, Future EUV/UV and Visible Space Astrophysics Missions and Instrumentation. SPIE, Bellingham, p. 129
Borucki W. J. et al., 2011, ApJ, 736, 19
Borucki W. J. et al., 2012, ApJ, 745, 120
Brott I., Hauschildt P. H., 2005, in Turon C., O'Flaherty K. S., Perryman M., eds, ESA SP- 576, The Three-Dimensional Universe with Gaia. ESA, Noordwijk, p. 565

Brown T. M., Latham D. W., Everett M. E., Esquerdo G. A., 2011, AJ, 142, 112
Bryden G. et al., 2006, ApJ, 636, 1098
Bryden G. et al., 2009, ApJ, 705, 1226
Burrows C. J., Krist J. E., Stapelfeldt K. R., WFPC2 Investigation Definition Team, 1995, BAAS, 27, 1329
Carpenter J. M. et al., 2009, ApJS, 181, 197
Castelli F., Kurucz R. L., 2003, in Piskunov N., Weiss W. W., Gray D. F., eds, Proc. IAU Symp. Vol. 210, Modelling of Stellar Atmospheres. Astron. Soc. Pac., San Francisco, p. 20
Chambers J. E., 2001, Icarus, 152, 205
Chambers J. E., Wetherill G. W., 1998, Icarus, 136, 304
Chen C. H. et al., 2006, ApJS, 166, 351
Ciardi D. R. et al., 2011, AJ, 141, 108
Clements D. L., Bendo G., Pearson C., Khan S. A., Matsuura S., Shirahata M., 2011, MNRAS, 411, 373
Dodson-Robinson S. E., Beichman C. A., Carpenter J. M., Bryden G., 2011, AJ, 141, 11
Doyle L. R. et al., 2011, Sci, 333, 1602
Fujiwara H. et al., 2010, ApJ, 714, L152
Fujiwara H., Onaka T., Yamashita T., Ishihara D., Kataza H., Fukagawa M., Takeda Y., Murakami H., 2012, ApJ, 749, L29
Gaidos E. J., 1999, ApJ, 510, L131
Gautier T. N., III et al., 2007, ApJ, 667, 527
Gomes R., Levison H. F., Tsiganis K., Morbidelli A., 2005, Nat, 435, 466
Hines D. C. et al., 2006, ApJ, 638, 1070
Holman M. J. et al., 2010, Sci, 330, 51
Howell S. B., Everett M. E., Sherry W., Horch E., Ciardi D. R., 2011, AJ, 42, 19
Høg E. et al., 2000, A&A, 355, L27
Jackson A. P., Wyatt M. C., 2012, MNRAS, in press
Jarrett T. H. et al., 2011, ApJ, 735, 112
Kalas P., Graham J. R., Clampin M., 2005, Nat, 435, 1067
Kalas P. et al., 2008, Sci, 322, 1345
Kennedy G. M. et al., 2012, MNRAS, 421, 2264
Kenyon S. J., Bromley B. C., 2005, AJ, 130, 269
Koerner D. W. et al., 2010, ApJ, 710, L26
Kóspál Á., Ardila D. R., Moór A., Ábrahám P., 2009, ApJ, 700, L73
Krivov A. V., Reidemeister M., Fiedler S., Löhne T., Neuhäuser R., 2011, MNRAS, 418, L15
La Franca F. et al., 2004, AJ, 127, 3075
Lawler S. M., Gladman B., 2012, ApJ, 752, 53
Lawler S. M. et al., 2009, ApJ, 705, 89
Lestrade J.-F., Wyatt M. C., Bertoldi F., Dent W. R. F., Menten K. M., 2006, A&A, 460, 733
Lestrade J.-F., Wyatt M. C., Bertoldi F., Menten K. M., Labaigt G., 2009, A&A, 506, 1455
Levison H. F., Morbidelli A., Vanlaerhoven C., Gomes R., Tsiganis K., 2008, Icarus, 196, 258
Lissauer J. J. et al., 2011a, Nat, 470, 53
Lissauer J. J. et al., 2011b, ApJS, 197, 8
Lisse C. M., Beichman C. A., Bryden G., Wyatt M. C., 2007, ApJ, 658, 584
Lisse C. M., Chen C. H., Wyatt M. C., Morlok A., Song I., Bryden G., Sheehan P., 2009, ApJ, 701, 2019
Lisse C. M. et al., 2012, ApJ, 747, 93
Lovis C. et al., 2006, Nat, 441, 305
Mamajek E. E., Hillenbrand L. A., 2008, ApJ, 687, 1264
Marois C., Macintosh B., Barman T., Zuckerman B., Song I., Patience J., Lafrenière D., Doyon R., 2008, Sci, 322, 1348
Matthews B. C. et al., 2010, A&A, 518, L135
Miville-Deschênes M.-A., Lagache G., 2005, ApJS, 157, 302
Moór A. et al., 2009, ApJ, 700, L25
Morbidelli A., Levison H. F., Tsiganis K., Gomes R., 2005, Nat, 435, 462
Moro-Martín A., Malhotra R., Bryden G., Rieke G. H., Su K. Y. L., Beichman C. A., Lawler S. M., 2010, ApJ, 717, 1123
Mouillet D., Larwood J. D., Papaloizou J. C. B., Lagrange A. M., 1997, MNRAS, 292, 896
Nesvorný D., Vokrouhlický D., Morbidelli A., 2007, AJ, 133, 1962
O'Donovan F. et al., 2006, ApJ, 651, L61
Papovich C. et al., 2004, ApJS, 154, 70
Phillips N. M., Greaves J. S., Dent W. R. F., Matthews B. C., Holland W. S., Wyatt M. C., Sibthorpe B., 2010, MNRAS, 403, 1089
Pilbratt G. L. et al., 2010, A&A, 518, L1
Raymond S. N. et al., 2011, A&A, 530, A62
Ribas Á., Merín B., Ardila D. R., Bouy H., 2012, A&A, 541, 38
Rieke G. H., Lebofsky M. J., 1985, ApJ, 288, 618
Rieke G. H. et al., 2005, ApJ, 620, 1010
Roberge A. et al., 2012, preprint (arXiv:1204.0025)
Siegler N., Muzerolle J., Young E. T., Rieke G. H., Mamajek E. E., Trilling D. E., Gorlova N., Su K. Y. L., 2007, ApJ, 654, 580
Skrutskie M. F. et al., 2006, AJ, 131, 1163
Skumanich A., 1972, ApJ, 171, 565
Smith B. A., Terrile R. J., 1984, Sci, 226, 1421
Smith R., Wyatt M. C., 2010, A&A, 515, A95
Smith R., Wyatt M. C., Haniff C. A., 2009, A&A, 503, 265
Song I., Zuckerman B., Weinberger A. J., Becklin E. E., 2005, Nat, 436, 363
Stark C. C., 2011, AJ, 142, 123
Su K. Y. L. et al., 2006, ApJ, 653, 675
Su K. Y. L. et al., 2009, ApJ, 705, 314
Tenenbaum P. et al., 2012, ApJS, 199, 24
Trilling D. E. et al., 2008, ApJ, 674, 1086
Verner G. A. et al., 2011, ApJ, 738, L28
Weinberger A. J., Becklin E. E., Song I., Zuckerman B., 2011, ApJ, 726, 72
Wright E. L. et al., 2010, AJ, 140, 1868
Wyatt M. C., 2008, ARA&A, 46, 339
Wyatt M. C., Smith R., Greaves J. S., Beichman C. A., Bryden G., Lisse C. M., 2007, ApJ, 658, 569
Wyatt M. C. et al., 2012, MNRAS, 424, 1206
Zuckerman B., Fekel F. C., Williamson M. H., Henry G. W., Muno M. P., 2008, ApJ, 688, 1345

SUPPORTING INFORMATION

Additional Supporting Information may be found in the online version of this article:

Table 1. The 271 *Kepler* stars with *WISE* 3–4 excesses.

Please note: Wiley-Blackwell are not responsible for the content or functionality of any supporting materials supplied by the authors. Any queries (other than missing material) should be directed to the corresponding author for the article.

This paper has been typeset from a TEX/LATEX file prepared by the author.